Ente per le Nuove tecnologie,
l'Energia e l'Ambiente

Ministero dello Sviluppo Economico

RICERCA SISTEMA ELETTRICO

HE-FUS3 Experimental Campaign for the Assessment of Thermal-Hydraulic Codes: Post-Test Analysis

Paride Meloni, Massimiliano Polidori

Report RSE/2009/89

Ente per le Nuove tecnologie,
l'Energia e l'Ambiente

Ministero dello Sviluppo Economico

RICERCA SISTEMA ELETTRICO

HE-FUS3 Experimental Campaign for the Assessment of Thermal-Hydraulic Codes: Post-Test Analysis

Paride Meloni, Massimiliano Polidori

Report RSE/2009/89

HE-FUS3 EXPERIMENTAL CAMPAIGN FOR THE ASSESSMENT OF THERMAL-HYDRAULIC CODES: POST-TEST ANALYSIS

Paride Meloni, Massimiliano Polidori (ENEA)

Aprile 2009

Report Ricerca Sistema Elettrico
Accordo di Programma Ministero dello Sviluppo Economico – ENEA
Area: Produzione e fonti energetiche
Tema: Nuovo Nucleare da Fissione
Responsabile Tema: Stefano Monti, ENEA

Table of Contents

Table of Contents

1. Introduction

2. Description of HE-FUS3 Experimental Program

2.1 Steady state conditions

2.2 LOFA transients

2.3 LOCA transients

3. Revision of the RELAP5 Model

3.1 Test Section Power

3.2 Loop Heat Losses

3.3 Economizer Efficiency

4. Post-test Calculations

4.1 Steady States

4.2 LOFA through Compressor Speed Reduction

4.3 LOFA through By-pass Valve Opening

4.4 LOCA at 30 bar Pressure

4.5 LOCA at 18 bar Pressure

5. References

1. Introduction

HE-FUS 3 is a helium facility that was designed and constructed at ENEA CR Brasimone in mid 90's for the thermal-mechanical testing of prototypical module assemblies of the DEMO reactor. Within the frame of the SP Safety (WP1) of the RAPHAEL Integrated Project, ENEA has offered the experimental data coming from a testing program carried out at the end of the nineties, for a benchmark exercise aimed at the validation of the system transient analysis codes for Very High Temperature Reactors (VHTR).

From the analyses performed with different codes [1] the large uncertainty affecting these experimental data has been highlighted. For this reason a new experimental campaign in the HE-FUS3 facility has been proposed [2] and conducted within the framework of the ENEA-MSE research program with the objective to provide a reliable experimental data base for the assessment of thermal-hydraulic codes used for HTR and VHTR design and safety analysis. This new campaign has also provided a better characterization of the loop, which will be of fundamental importance for the future modeling activity of the facility.

The numerical simulations have been carried out with the RELAP5 model used for the pre-test phase with the main objective to identify the necessary code developments and model improvements that are planned during the second year of the ENEA-MSE research program. Besides this, the post-test analysis has provided an evaluation of the experimental transients performed that has allowed identifying the needs in term of further tests and additional instrumentation for the future experimental programs.

2. Description of HE-FUS3 Experimental Program

The experimental program, that was conducted in the HE-FUS3 facility (Fig. 2.1) in the time period between November 2008 and March 2009, was carried out in agreement with the test matrix defined with the pre-test activity [2] and following as much as possible the specifications drawn up from the pre-test calculations.
On the whole, the performed test matrix has included 7 different steady state conditions, 2 LOFA transients and two LOCA transients that will be shortly described in the following paragraphs referring to the experimental data report [3] for a more detailed description.

2.1 Steady state conditions

During the He-FUS3 experimental program the reference steady state conditions for the foreseen transient tests were reached by means of a step-by-step procedure increasing compressor speed and Test Section power. This approach allowed acquiring a complete information for 5 different steady states at relatively high pressure that represent an exhaustive information for the loop characterization. Besides of these, other 2 further steady states at lower pressure were acquired during the blow down phase of the loop, when the pressure was decreased through two LOCA transients.

The experimental data related to the different transients were recorded after at least 15 hour of constant conditions in the loop, as required in the specifications drawn by the pre-test analysis, in order to guarantee that “real” steady state conditions were established in the loop.

Table 2.1 reports some relevant parameters of the steady states that were obtained by means of different combinations of the following parameters controlled during the HE-FUS3 operation: compressor speed, test section power and expansion tank pressure.

Steady state	Tank Pressure	Test Section power	Compressor Speed	Loop Mass Flowrate	Max Helium Temperature
	bar	kW	rpm	Kg/h	°C
First step start-up	35	44	11000	480	293
Second step start-up	34	44	13500	585	269
Third step start-up	35	85	13500	566	401
Forth step start-up	34	104	13500	560	422
Additional step start-up	32	85	11000	430	424
Low pressure steady state 1	20	82	13500	323	469
Low pressure steady state 2	18	41	13500	296	379

Tab. 2.1 – HE-FUS3 steady states

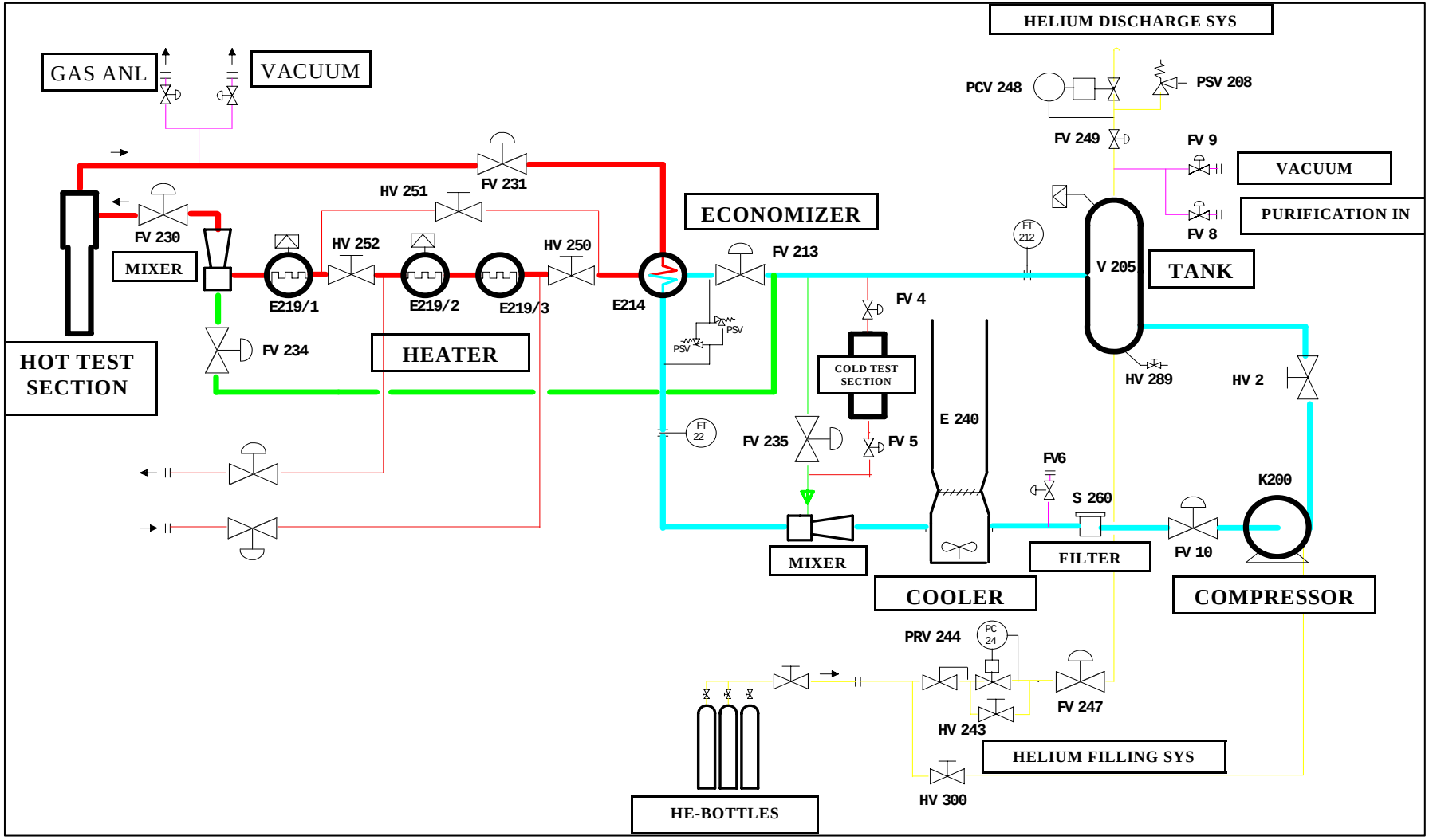

Fig. 2.1 – HE-FUS3 P&I

The status of the loop is recorded through a series of 36 measurements (Fig. 2). that are provided for each steady state above described and for the most part acquired during the transient tests. The description of these 36 measurements is given in the following:

TR 218 – Economizer Outlet Temperature (Hot Side) [°C]
TR 215 – Economizer Inlet Temperature (Cold Side) [°C]
TR 217 – Economizer Inlet Temperature (Hot Side) [°C]
TR 216 – Economizer Outlet Temperature (Cold Side) [°C]
FIC 228X – Economizer Outlet Mass Flowrate (Hot Side) [kg/h]
TR 239 – Cold Mixer Outlet Temperature [°C]
TIC 242X – Air Cooler Outlet Temperature (Helium) [°C]
TR 267 - Air Cooler Inlet Temperature (Air) [°C]
TR 266 - Air Cooler Outlet Temperature (Air) [°C]
TR 202 - Compressor Inlet Temperature [°C]
TR 211 – Tank Temperature [°C]
TR 204 - Compressor Outlet Temperature [°C]
PDT 201 – In-Out Compressor Differential Pressure [bar]
FIC212X - Compressor Outlet Mass Flowrate [kg/h]
ZR 235 – Opening of Valve V235 (%)
ZR 213 – Opening of Valve V213 (%)
ZR 234 – Opening of Valve V234 (%)
TR 220 – Heater E219/3 Inlet Temperature [°C]
TR 221 – Heater E219/3 Outlet Temperature [°C]
TR 226 – Heater E219/3 Rod Temperature [°C]
TIC 222X - Heater E219/2 Outlet Temperature for Power Regulation [°C]
TR 225 – Heater E219/2 Rod Temperature [°C]
TIC 223X - Heater E219/1 Outlet Temperature for Power Regulation [°C]
TR 224 – Heater E219/1 Rod Temperature [°C]
TIC 232X – Test Section Inlet Temperature for Regulation Valves V234/V213 [°C]
TR 233 - Test Section Outlet Temperature [°C]
TR 241 - Compressor Inlet Temperature for Protection System [°C]
TR 236 - Heater E219/1 Inlet Temperature for Protection System [°C]
TR 297 - Heater E219/2 Inlet Temperature for Protection System [°C]
ST 270 – Compressor Speed [rpm 10^{-2}]
PR 298 – Compressor Inlet Pressure [bar]
PR 206 – Tank Pressure [bar]
PR 227 – Test Section Inlet Pressure [bar]
PDR 229 – In-Out Test Section Differential Pressure [bar]
TE 101 – Test Section Inlet Temperature [°C]
TE 201 – Test Section Outlet Temperature [°C]

The distribution of temperature along the loop should be completely characterized through 17 thermocouples properly located. Two of these thermocouples were unavailable during the experimental campaign: TR233 located at the Test Section outlet and TR204 located at the compressor outlet. Whereas the temperature recorded by the TR233 is also provided by the thermocouples TR102 implemented directly within the Test Section, there is no equivalent instrument for the TR204.

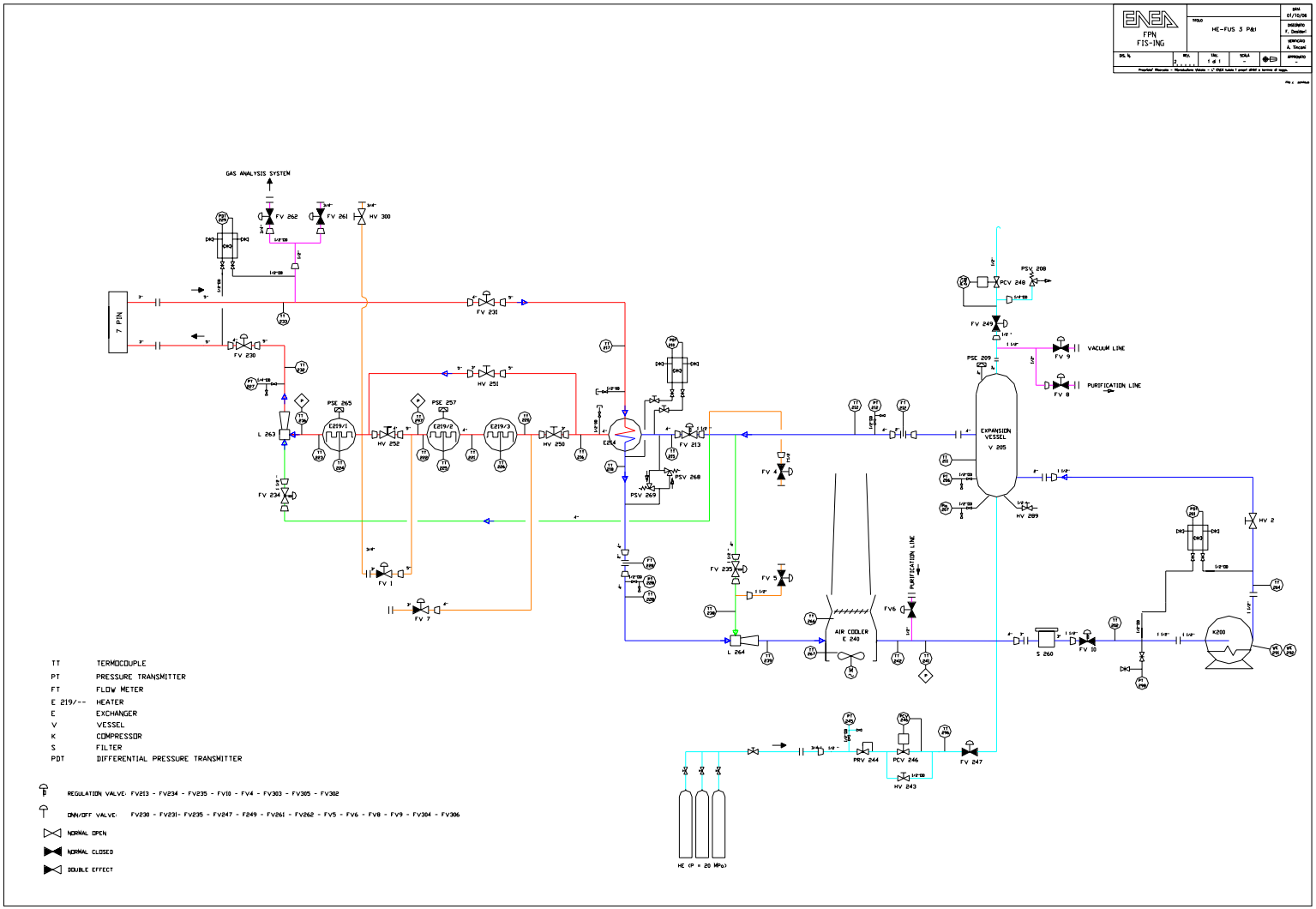

Fig. 2.2 – HE-FUS3 Instrumentation Map

The closer thermocouple recorded by the acquisition system is TR211 located in the tank but not acquired during the transient tests. So it has been decided to refer directly to the thermocouple TR215 at the inlet of the economizer, having in mind that a difference of a few degrees due to the heat losses and gas expansion is expected respect to the actual temperature at the compressor outlet.

Some loop positions are provided with two or more instruments that should give very close temperatures. In general that is confirmed by the recorded data, except for two cases: TR218 and TR239 at the economizer hot side outlet differ of 3-4 °C in all steady states, TR242-TR241 , at the air cooler outlet are constantly higher of 4-5 °C respect to TR202.

In the previous assessment activity performed on the HE-FUS3 experimental data [1] it was highlighted the necessity, for the future campaigns, to implement a more reliable system for the measurement of the 7-pin power and to acquire more information from the thermocouples already embedded in the 7-pin test section (Fig. 3). Both this actions were accomplished during 2008. Two independent measurement of the power are available: one related to the identical pins 1 to 6 the other dedicate to the "hot" pin 7. In the tests the peak factor ranged from 1.4 to 2 depending on the steady state conditions. Moreover, except for the lower position of the pin 7, 27 thermocouple signals have been acquired during the tests.

SENSOR	RESISTOR	SENSOR HEIGHT
TE112	R1	250
TE110	R1	750
TE111	R1	1250
TE103	R1	1750
TE114	R2	250
TE104	R2	750
TE113	R2	1250
TE115	R2	1750
TE201	R3	250
TE118	R3	750
TE116	R3	1250
TE117	R3	1750
TE210	R4	250
TE212	R4	750
TE202	R4	1250
TE211	R4	1750
TE203	R5	250
TE214	R5	750
TE215	R5	1250
TE312	R5	1750
TE217	R6	250
TE216	R6	750
TE204	R6	1250
TE218	R6	1750
NA	R7	250
TE310	R7	750
TE304	R7	1250
TE301	R7	1750

Thermocouples location

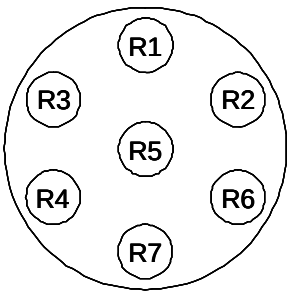

Resistor arrangement

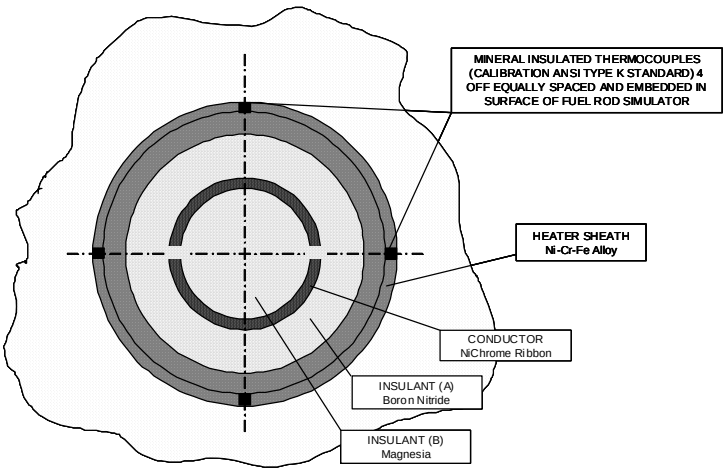

Resistor section

Fig. 2.3 –Test Section Thermocouples Location

A part from the build-up of a data-base for the code-to-data assessment of the thermal-hydraulic system codes, the acquired steady states are essential for an exhaustive characterization of the loop heat losses and intermediate helium-helium heat exchanger (economizer) at different loop conditions. These points were recognized to be necessary for a correct numerical modeling of the HE-FUS3 facility.

The heat losses of the HE-FUS3 loop have been estimated by means of enthalpy balances based on measured helium temperatures and mass flowrates. Their distribution in the main parts of the loop is reported in Table 2.2

The estimated heat losses in the whole loop are quite coherent in all different conditions, in fact the values range from 15 to 26 kW depending mainly on the power level. For a few steady states some discrepancies are present in their distribution between the different parts of the loop. This fact is likely connected with the uncertainty that affect the temperature measurements used in the enthalpy balances. Concerning only the thermocouples accuracy the uncertainty was evaluated in about 3 °C in a previous work [4], as a consequence considering the uncertainty range on both the instruments used for the balances the uncertainty in the power could be up to about 6 kW.

Steady state	**Heat Losses (kW)**				
	Test Section	**Economizer**	**Heaters**	**Cold zone**	**Total**
First step start-up	5.2	4,5	3,5	1,7	14.9
Second step start-up	5.2	4	4,2	1.8	15.2
Third step start-up	5.8	8	7.5	1.8	23.
Forth step start-up	6.5	6.5	9	1.9	26.1
Additional step start-up	11.2	4.1	8.8	1.1	25.2
Low pressure steady state 1	8	1	13.7	1	23.7
Low pressure steady state 2	3.5	5.7	4.7	1.1	15

Tab. 2.2 – Heat Losses Distribution in the different steady states

The efficiency of a heat exchanger, defined as the ratio between the power actually exchanged and the maximum ideal value of the exchanged power, is an useful information about the heat exchanger performance. The measured temperatures and mass flowrates on both sides of the economizer have allowed to estimate by means of the formula (1) the efficiency of this component at the different conditions.

$$\varepsilon = \frac{Q_{scambiato}}{Q_{Max\ scambiabile}} = \frac{(m\,c_p)_c(T_{ci} - T_{cu})}{(m\,c_p)_{min}(T_{ci} - T_{fi})} = \frac{(m\,c_p)_f(T_{fi} - T_{fu})}{(m\,c_p)_{min}(T_{ci} - T_{fi})} \qquad (1)$$

$Q_{scambiato}$ is the power actually exchanged; the $Q_{Max\ scambiabile}$ is the max ideal value of the exchanged power; $m \cdot c_p$ is the product between mass flowrate and specific heat calculated for the hot (*c*) and cold (*f*) fluid; T_{ci}, T_{cu} etc. are the fluid temperatures calculated for hot/cold fluid and at inlet/outlet of the exchanger.

In table 2.3 the calculated values of efficiency are reported for each steady state together with the deviation deriving from the calculation on primary (cold helium) and secondary (hot helium side). This parameter is of great importance to evaluate the suitability of the numerical model adopted for the simulation of the economizer.

One can notice that the efficiency of the economizer, in general, depends remarkably from the helium flow conditions. In particular, the gas velocity seems to be the most important parameter that influences the economizer performance.

	Max Power	**Actual Power**	**% Deviation**	**Efficiency**
First step start-up	146.5	114.2	2,5	0,78
Second step start-up	147.5	114.6	3	0.78
Third step start-up	213.9	179.4	4.5	0.84
Forth step start-up	203.5	178.6	4.3	0.88
Additional step start-up	171.8	146.7	3.6	0.75
Low pressure steady state 1	121.2	109	4.1	0.9
Low pressure steady state 2	125.4	96.6	3.1	0.77

Tab. 2.3 – Economizer efficiency in the different steady states

2.2 LOFA transients

Two LOFA transients with a different dynamic behavior of the loop have been carried out in the facility according to the calculations performed in the pre-test analysis.

The first LOFA transient has concerned a quite slow reduction of the TS mass flow rate through the reduction of the compressor speed in order to simulate the behavior of a helium loop following a compressor coast down event. The transient has started from the steady state conditions reached in the forth step of the start-up: 34 bar pressure, 104 kW power and 13500 rpm compressor speed that has corresponded to 560 kg/h.

The transient was performed by slowing down the compressor from 13500 rpm to 7995 rpm in 105 s. After about 35 minutes in low flow conditions the initial speed of the compressor was restored in 120 s.

The main boundary condition of the transient are summarized in table 2.4

Initial and Boundary Conditions	Value	Time (s)
Initial Pressure (bar)	34	0.
TS Electrical Power (kW)	104.	0.
Initial Compressor Speed (rpm)	13500.	0.
Compressor speed start decreasing (rad/s)	13500.	453.
Compressor speed stop decreasing (rad/s)	7995.	558.
Compressor speed start increasing (rad/s)	7995.	2723.
Compressor speed stop increasing (rad/s)	13500.	2843.
TS Helium Inlet Temperature (°C)	300.	All transient
Air Cooler Helium Outlet Temperature (°C)	65.-62	According exp. values
TS Electrical Power	104.- 107.8	According exp. values

Tab. 2.4 – Initial and boundary conditions for the LOFA through compressor speed reduction

The second LOFA transient has been started with a complete opening of the valve F235, which allows the helium to bypass the hot part of the loop, in order to test a sharper reduction of the TS mass flow rate. In order to avoid too critical temperatures in the TS pins the transient started from initial temperatures lower respect to those of the previous transient. The initial steady state conditions are quite similar to the conditions reached in the third step of the start-up: 32 bar pressure, 81 kW power and 13500 rpm compressor speed that has corresponded to 510 kg/h.

The main initial and boundary conditions of the transient are summarized in table 2.5

Initial and Boundary Conditions	Value	Time (s)
Initial Pressure (bar)	32	0.
Initial TS Electrical Power (kW)	81.1	0.
Compressor Speed (rpm)	13500.	All transient
By-pass Valve 235 (% opening)	0.	344.
By-pass Valve 235 (% opening)	1.	354.
By-pass Valve 235 (% opening)	1.	1505.
By-pass Valve 235 (% opening)	0.	1515.
TS Helium Inlet Temperature (°C)	300.	All transient
Air Cooler Helium Outlet Temperature (°C)	65.-64	According exp. values
TS Electrical Power	81.1 – 82.4	According exp. values

Tab. 2.5 – Initial and boundary conditions for the LOFA through by-pass valve opening

2.2 LOCA transients

Two LOCA transients with a different loop pressure have been carried out in the facility according to the calculations performed in the pre-test analysis.

Both LOCAs were simulated in the pre-tests analysis by opening a valve of 75 mm^2 area (equivalent to about 1 % of the cold pipe flow area) in the tank component. Due to the fact the valves present on this component are smaller (1/2") the break occurrence has been simulated by the simultaneous opening of three valves with an equivalent area of 150 mm^2. In this way the flow area is about twice the pre-test value, but it is worth to underlined that the presence of discharge piping having the same flow area of the valves and a total length of about 5 m reduces notably the discharged mass flow.

The first LOCA transient has started from steady state conditions similar to the conditions reached in the third step of the start-up: 31 bar pressure, 81 kW power and 13500 rpm compressor speed that has corresponded to 497 kg/h.

The LOCA event has been simulated opening all the three valves on the tank for 3 minutes that has corresponded to a depressurization of about 12 bar.

The main boundary condition of the transient are summarized in table 2.6

Initial and Boundary Conditions	Value	Time (s)
Initial Pressure (bar)	31.0	0.
TS Electrical Power (kW)	81.	0.
Initial Compressor Speed (rpm)	1350.	All transient
Break Opening (m^2)	0.0151 10^{-3}	0.
Break Closure (m^2)	0.	180.
TS Helium Inlet Temperature (°C)	300.	All transient
TS Electrical Power (kW)	81 - 84	According exp. values
Air Cooler Helium Outlet Temperature (°C)	65. – 58.	According exp. values

Tab. 2.6 – Initial and boundary conditions for the LOCA at higher pressure

The second LOCA transient has started from the loop pressure reached at the end of the previous LOCA transient at a reduced power (low pressure steady state nr 2): 18 bar pressure, 41.5 kW power and 13500 rpm compressor speed that has corresponded to 296 kg/h.

The LOCA event has been simulated opening all the three valves on the tank for 3 minutes that has corresponded to a depressurization of about 11 bar.

The main boundary condition of the transient are summarized in table 2.6

Initial and Boundary Conditions	Value	Time (s)
Initial Pressure (bar)	18.0	0.
TS Electrical Power (kW)	41.5	0.
Initial Compressor Speed (rpm)	1350.	All transient
Break Opening (m^2)	$0.0151\ 10^{-3}$	0.
Break Closure (m^2)	0.	180.
TS Helium Inlet Temperature (°C)	< 300	All transient
TS Electrical Power (kW)	41.5 – 42.9	According exp. values
Air Cooler Helium Outlet Temperature (°C)	44. – 23.	According exp. values

Tab. 2.2 – Initial and boundary conditions for the LOCA at lower pressure

3. Revision of the RELAP5 Model

In the pre-test report [2] the RELAP5 model of the loop (fig 3.1) was widely described paying a particular attention to the main modeling assumptions. Some of these assumptions, in particular related to loop heat losses, economizer and compressor, required a calibration process against pre-existing experimental data poorly validated. Due to their large effect on the calculation results it has been considered essential to repeat the process against one of the present steady state in order to set up the loop model for the post-test calculations.

As a reference steady state for the calibration process it has been selected the third step start-up one, as two of the transient conducted in the loop started from these conditions.

2.1 Loop Heat Losses

As explained in [2] all the hydraulics components of the loop are thermally coupled with the environment in order to simulate the actual thermal energy losses.

In order to simulate the high heat losses experimented in the hot portion of the loop (Test Section, Economizer and Heater) a high fictitious values for the thermal conductivity of the rock wool (insulating material) were adopted in the RELAP5 model. These values have been re-calibrated against the heat losses of the reference steady state, which have been computed by means of enthalpy balance on the different zones.

Table 3.1 shows the values used in the pre-test calculations and the new ones. It can be noticed that only for the economizer the heat losses have been estimated on the basis of the new experimental data considerably larger than pre-calculated so the thermal conductivity of the rock wool has been almost doubled.

In table 3.2 are reported the heat losses calculated with the new values in comparison with the estimate ones. The agreement is not still perfect especially for the economizer, however it is considered acceptable taking into account the uncertainty on the experimental temperatures used in the enthalpy balances (for instance 3 °C count about for 2 kW) and therefore on the heat losses themselves.

Part of the Loop	Pre-test calculations	Post-test calculations λ
	(w/m °C)	(w/m °C)
Cold zone	nominal values	nominal values
Economizer	0.35	0.65
Electrical Heaters	0.35	0.27
Test Section	0.25	0.25

Table 3.2 – Insulator Material Thermal Conductivity

Part of the Loop	Experimental (Estimated)	Post-test calculations λ
	(kW)	(kW)
Cold zone	1.7	2.3
Economizer	8.	6.4
Electrical Heaters	7.5	8
Test Section	5.8	5.9
Total	23.	21.6

Table 3.3 – Experimental and Calculated Heat Losses

3.2 Economizer

A correct simulation of the performance of this component is fundamental for a correct prediction of the temperature distribution in the hot part of the loop as well as for a correct operation of the control system. In Reference [2] it was recognized the inadequacy of the standard RELAP5 correlation (Dittus-Boelter) for the heat transfer coefficient in the shell side of the economizer. In order to reproduce the expected performance of the heat thermal exchange the common place approach of reducing appropriately the heating diameter was applied to the economizer shell side. The value introduced in the model (1.63 10^{-3} m against 1.82 10^{-2} m) allowed an acceptable prediction of the pre-exiting experimental data on the economizer temperatures

This heating diameter has been revised in order to obtain from the RELAP5 model a good estimation of the economizer efficiency (see § 2.1) at the reference steady state condition. A slightly larger value than the previous adopted (2.2 10^{-3} m instead of 1.63 10^{-3} m) allows in the calculation to find an efficiency very close to the estimated one (0.833 against 0.838).

3.3 Compressor

In order to provide for the lack of a specific compressor model in RELAP5, lots of work was made during the pre-test activity to construct a set of homologous curves for the rotating pump component that allowed it to simulate the compressor behaviour in the range of conditions planned for the experiment. To this end characterisation tests both for head and torque performed on 1998 were used.

The assessment on the reference steady state mass flowrate, head and torque shows that these old data were completely unreliable, in fact the compressor performance are well higher than the pre-calculated ones. This mean that a new set of homologous curves has to be constructed on the basis of the new data available.

This work is planned as a follow up of the current activity within the framework of the second year of the ENEA-MSE research program. At present, in order to overcome the poor prediction of the compressor performance in the present calculations an “ad hoc” regulation will be used in the different transients.

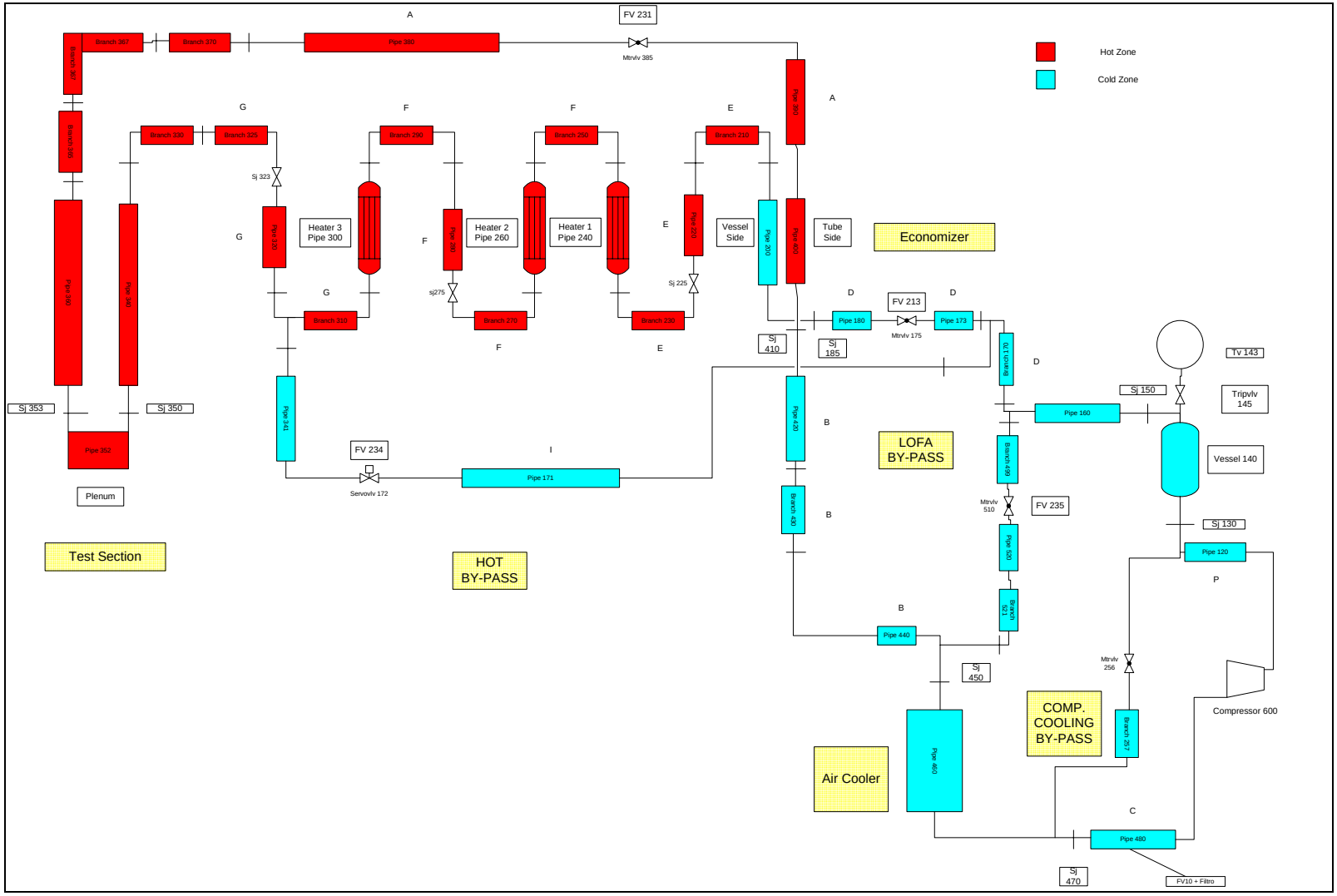

Fig. 3.1 – RELAP5 Nodalization Scheme of HE-FUS

4. Post-Test Calculations

4.1 Steady state conditions

The steady state loop conditions reported in Tab. 2.1 have been re-calculated with the RELAP5 model set up for the pre-test activity with some modeling assumption updated as described in the previous paragraph.

For each steady state the boundary conditions imposed and the main loop parameters calculated by the code are compared with the available experiment values and reported in Tables 4.1 to 4.7 . The description of these available measurements has been reported in §. 2.1.

Due to the poor performance of the compressor model the loop mass flowrate has been imposed by means of a boundary condition, therefore the comparison of the compressor speed does not make sense. The comparison is mainly related to the temperature distribution along the loop and inside the seven-pin test section. Concerning the measurements on the different pins those related to the pins 1 and 2 are not used because some discrepancy showed from the recorded data (unphysical decrease of the pin temperature with the elevation).

The calculations show a good agreement with the experimental power absorbed in the hot zone of the loop, correct that is a sign of a correct prediction of the heat losses as reported in Tab. 4.8. The minor differences are explained by a slight influence of the loop temperature (heat losses increase with the temperature) not taken into account in the numerical model. Anyway, this dependence, which could be considered in an upgraded model, causes discrepancy on the temperatures comparable with the uncertainty on the experimental data.

The situation is quite different in the calculation of the economizer performance as showed in Tab. 4.9. In fact, the efficiency that has been exactly tuned for the third step start-up steady state is quite dependent from the loop conditions. As a consequence the calculated temperatures in the hot part of the loop are not so in agreement with the experimental data for all steady state conditions. In particular, one can notice that the steady state at lower pressure that the reference one present temperatures higher than 10 °C or more. The present model of the economizer seems to be suitable to take into account different loop mass flowrates, whereas it has to be improved to take into account correctly the strong dependence on the temperature of the physical property of the helium.

Concerning the 7-pin test section the discrepancy between calculated and experimental temperatures at the different elevations for both the averaged one on the 6 pins and the hot pin are for the most around 10 °C. This difference is quite acceptable, also considering that the lack of information about the exact positions of the thermocouples and the mixing effect between central and peripheral channels is responsible for a simplified and averaged model. This information would be fundamental to deduce for example, the effect of the strong variation of the helium physical properties on the heat transfer performance thus allowing an improving of the TS model. For a few steady states the experimental hot pin temperature at 1,25 m (TE 304) that has resulted incoherent with the other temperatures recorded is highlighted in red.

Controlled parameter	Experimental Value		RELAP5 boundary condition	
Loop Pressure (bar)	35		35	
TS Electrical Power (kW)	44		44	
Loop Mass Flowrate (kg/s)	0,134-0,133		0,1335	
Max TS Helium Inlet Temperature	300		300	
Air Cooler Outlet Temperature	65		65	
Calculated Parameter	**HE-FUS3 Tag**	**Experimental Value**	**RELAP Reference**	**Calculated Value**
Total Pressure Drop (bar)	PD201	1.31	cntrlvar 40	1.35
TS Pressure Drop (bar)	PD229	0.405	cntrlvar 41	0.427
Valve F234 % Opening	ZT234	0.	vlvarea 172	0.
E214 Inlet Cold Side Temperature (°C)	TR215	77.	cntrlvar 215	84.
E214 Out Cold Side Temperature (°C)	TR216	240.	cntrlvar 216	244.
E219/1 Outlet Temperature (°C)	TR223-TR236	235.	cntrlvar 223	234.
TS Outlet Temperature	TE102	293.	cntrlvar225	295.5
E214 Inlet Hot Side Temperature (°C)	TR217	289.	cntrlvar 217	293..
E214 Outlet Hot Side Temperature (°C)	TR218-TR239	122. – 124.	cntrlvar 218	128.
Compressor Outlet Temperature (°C)	TR204	77.	cntrlvar 204	86.5
Average Pin Temperature at 0.25 m High (°C)	TE201, TE203, TE210, TT217	290.	cntrlvar 210	298.
Average Pin Temperature at 0.75 m High (°C)	TE118, TE212, TE214, TE216	306.	cntrlvar 211	315.
Average Pin Temperature at 1.25 m High (°C)	TE116, TE202, TE204, TE215	337.	cntrlvar 212	328.
Average Pin Temperature at 1.75 m High (°C)	TE117, TE211, TE213, TE218	348.	cntrlvar 213	344.
Hot Pin Temp. at 0.75 m High (°C)	TE310	344.	cntrlvar 215	361.
Hot Pin Temp. at 1.25 m High (°C)	TE304	382.	cntrlvar 216	374.
Hot Pin Temp. at 1.75 m High (°C)	TE301	401.	cntrlvar 217	390.

Table 4.1 – First step start-up Steady State Experiment-Calculation Comparison

Controlled parameter	Experimental Value		RELAP5 boundary condition	
Loop Pressure (bar)	34.		34.	
TS Electrical Power (kW)	44.		44.	
Loop Mass Flowrate (kg/s)	0.1625-0.164		0.163	
Max TS Helium Inlet Temperature	300.		300.	
Air Cooler Outlet Temperature	65.		65.	
Calculated Parameter	**HE-FUS3 Tag**	**Experimental Value**	**RELAP Reference**	**Calculated Value**
Total Pressure Drop (bar)	PD201	1.91	cntrlvar 40	2.01
TS Pressure Drop (bar)	PD229	0.662	cntrlvar 41	0.607
Valve F234 % Opening	ZT234	0.	vlvarea 172	0.
E214 Inlet Cold Side Temperature (°C)	TR215	92.	cntrlvar 215	94.
E214 Out Cold Side Temperature (°C)	TR216	226.	cntrlvar 216	215.
E219/1 Outlet Temperature (°C)	TR223-TR236	221. -223.	cntrlvar 223	209.
TS Outlet Temperature	TE102	269.	cntrlvar225	257.
E214 Inlet Hot Side Temperature (°C)	TR217	267.	cntrlvar 217	255..
E214 Outlet Hot Side Temperature (°C)	TR218-TR239	129. – 130.	cntrlvar 218	130.
Compressor Outlet Temperature (°C)	TR204	92.	cntrlvar 204	97.
Average Pin Temperature at 0.25 m High (°C)	TE201, TE203, TE210, TT217	267.	cntrlvar 210	260.
Average Pin Temperature at 0.75 m High (°C)	TE118, TE212, TE214, TE216	279.	cntrlvar 211	274.
Average Pin Temperature at 1.25 m High (°C)	TE116, TE202, TE204, TE215	303.	cntrlvar 212	284.
Average Pin Temperature at 1.75 m High (°C)	TE117, TE211, TE213, TE218	312.	cntrlvar 213	297.
Hot Pin Temp. at 0.75 m High (°C)	TE310	310.	cntrlvar 215	316.
Hot Pin Temp. at 1.25 m High (°C)	TE304	346.	cntrlvar 216	326.
Hot Pin Temp. at 1.75 m High (°C)	TE301	358.	cntrlvar 217	339.

Table 4.2 – Second step start-up Steady State Experiment-Calculation Comparison

Controlled parameter	Experimental Value		RELAP5 boundary condition	
Loop Pressure (bar)	35.		35.	
TS Electrical Power (kW)	85.		85.	
Loop Mass Flowrate (kg/s)	0.159-0.157		0.158	
Max TS Helium Inlet Temperature	300.		300.	
Air Cooler Outlet Temperature	65.		65.	
Calculated Parameter	**HE-FUS3 Tag**	**Experimental Value**	**RELAP Reference**	**Calculated Value**
Total Pressure Drop (bar)	PD201	1.97	cntrlvar 40	1.90
TS Pressure Drop (bar)	PD229	0.670	cntrlvar 41	0.685
Valve F234 % Opening	ZT234	26.	vlvarea 172	32.
E214 Inlet Cold Side Temperature (°C)	TR215	93.	cntrlvar 215	91.5
E214 Out Cold Side Temperature (°C)	TR216	342.	cntrlvar 216	341.5
E219/1 Outlet Temperature (°C)	TR223-TR236	333. -334.	cntrlvar 223	330.5
TS Outlet Temperature	TE102	398.	cntrlvar225	401.
E214 Inlet Hot Side Temperature (°C)	TR217	397.	cntrlvar 217	396.5
E214 Outlet Hot Side Temperature (°C)	TR218-TR239	172. – 176.	cntrlvar 218	171.5
Compressor Outlet Temperature (°C)	TR204	93.	cntrlvar 204	94.5
Average Pin Temperature at 0.25 m High (°C)	TE201, TE203, TE210, TT217	400.	cntrlvar 210	409.
Average Pin Temperature at 0.75 m High (°C)	TE118, TE212, TE214, TE216	417.	cntrlvar 211	436.
Average Pin Temperature at 1.25 m High (°C)	TE116, TE202, TE204, TE215	466.	cntrlvar 212	457.
Average Pin Temperature at 1.75 m High (°C)	TE117, TE211, TE213, TE218	501.	cntrlvar 213	483.
Hot Pin Temp. at 0.75 m High (°C)	TE310	458.	cntrlvar 215	473.
Hot Pin Temp. at 1.25 m High (°C)	TE304	514.	cntrlvar 216	494.
Hot Pin Temp. at 1.75 m High (°C)	TE301	525.	cntrlvar 217	519.

Table 4.3 – Third step start-up Steady State Experiment-Calculation Comparison

Controlled parameter	Experimental Value		RELAP5 boundary condition	
Loop Pressure (bar)	34.		34.	
TS Electrical Power (kW)	104.		104.	
Loop Mass Flowrate (kg/s)	0.1565-0.1575		0.157	
Max TS Helium Inlet Temperature	300.		300.	
Air Cooler Outlet Temperature	64.		64.	
Calculated Parameter	**HE-FUS3 Tag**	**Experimental Value**	**RELAP Reference**	**Calculated Value**
Total Pressure Drop (bar)	PD201	1.92	cntrlvar 40	1.89
TS Pressure Drop (bar)	PD229	0.681	cntrlvar 41	0.718
Valve F234 % Opening	ZT234	42.	vlvarea 172	52.
E214 Inlet Cold Side Temperature (°C)	TR215	93.	cntrlvar 215	91.5
E214 Out Cold Side Temperature (°C)	TR216	372.	cntrlvar 216	377.5
E219/1 Outlet Temperature (°C)	TR223-TR236	361. -361.	cntrlvar 223	364
TS Outlet Temperature	TE102	423.	cntrlvar225	422.
E214 Inlet Hot Side Temperature (°C)	TR217	418.	cntrlvar 217	420.
E214 Outlet Hot Side Temperature (°C)	TR218-TR239	192. – 195.	cntrlvar 218	194.
Compressor Outlet Temperature (°C)	TR204	93.	cntrlvar 204	95.5
Average Pin Temperature at 0.25 m High (°C)	TE201, TE203, TE210, TT217	429.	cntrlvar 210	437.
Average Pin Temperature at 0.75 m High (°C)	TE118, TE212, TE214, TE216	442.	cntrlvar 211	470.
Average Pin Temperature at 1.25 m High (°C)	TE116, TE202, TE204, TE215	504.	cntrlvar 212	495.
Average Pin Temperature at 1.75 m High (°C)	TE117, TE211, TE213, TE218	536.	cntrlvar 213	527.
Hot Pin Temp. at 0.75 m High (°C)	TE310	489.	cntrlvar 215	502.
Hot Pin Temp. at 1.25 m High (°C)	TE304	560.	cntrlvar 216	527.
Hot Pin Temp. at 1.75 m High (°C)	TE301	554.	cntrlvar 217	559.

Table 4.4 – Fourth step start-up Steady State Experiment-Calculation Comparison

Controlled parameter	Experimental Value		RELAP5 boundary condition	
Loop Pressure (bar)	32.		32.	
TS Electrical Power (kW)	83.		83.	
Loop Mass Flowrate (kg/s)	0.120		0.120	
Max TS Helium Inlet Temperature	300.		300.	
Air Cooler Outlet Temperature	65.		65.	
Calculated Parameter	**HE-FUS3 Tag**	**Experimental Value**	**RELAP Reference**	**Calculated Value**
Total Pressure Drop (bar)	PD201	1.22	cntrlvar 40	1.20
TS Pressure Drop (bar)	PD229	0.441	cntrlvar 41	0.452
Valve F234 % Opening	ZT234	35.	vlvarea 172	51.
E214 Inlet Cold Side Temperature (°C)	TR215	79.	cntrlvar 215	83.5
E214 Out Cold Side Temperature (°C)	TR216	364.	cntrlvar 216	382.
E219/1 Outlet Temperature (°C)	TR223-TR236	350. -351.	cntrlvar 223	364
TS Outlet Temperature	TE102	424.	cntrlvar225	426.
E214 Inlet Hot Side Temperature (°C)	TR217	419.	cntrlvar 217	423.
E214 Outlet Hot Side Temperature (°C)	TR218-TR239	178. – 180.	cntrlvar 218	182.
Compressor Outlet Temperature (°C)	TR204	79.	cntrlvar 204	86.0
Average Pin Temperature at 0.25 m High (°C)	TE201, TE203, TE210, TT217	425.	cntrlvar 210	437.
Average Pin Temperature at 0.75 m High (°C)	TE118, TE212, TE214, TE216	439.	cntrlvar 211	471.
Average Pin Temperature at 1.25 m High (°C)	TE116, TE202, TE204, TE215	496.	cntrlvar 212	498.
Average Pin Temperature at 1.75 m High (°C)	TE117, TE211, TE213, TE218	536.	cntrlvar 213	530.
Hot Pin Temp. at 0.75 m High (°C)	TE310	502.	cntrlvar 215	513.
Hot Pin Temp. at 1.25 m High (°C)	TE304	566.	cntrlvar 216	539.
Hot Pin Temp. at 1.75 m High (°C)	TE301	563.	cntrlvar 217	571.

Table 4.5 – Additional start-up Steady State Experiment-Calculation Comparison

Controlled parameter	Experimental Value		RELAP5 boundary condition	
Loop Pressure (bar)	20.		20.	
TS Electrical Power (kW)	83.		83.	
Loop Mass Flowrate (kg/s)	0.09		0.09	
Max TS Helium Inlet Temperature	300.		300.	
Air Cooler Outlet Temperature	65.		65.	
Calculated Parameter	**HE-FUS3 Tag**	**Experimental Value**	**RELAP Reference**	**Calculated Value**
Total Pressure Drop (bar)	PD201	1.16	cntrlvar 40	1.13
TS Pressure Drop (bar)	PD229	0.435	cntrlvar 41	0.437
Valve F234 % Opening	ZT234	53.	vlvarea 172	67.
E214 Inlet Cold Side Temperature (°C)	TR215	91.	cntrlvar 215	94.
E214 Out Cold Side Temperature (°C)	TR216	417.	cntrlvar 216	438.
E219/1 Outlet Temperature (°C)	TR223-TR236	388. - 389.	cntrlvar 223	406.
TS Outlet Temperature	TE102	470.	cntrlvar225	469.
E214 Inlet Hot Side Temperature (°C)	TR217	461.	cntrlvar 217	465.
E214 Outlet Hot Side Temperature (°C)	TR218-TR239	222. – 223.	cntrlvar 218	221.
Compressor Outlet Temperature (°C)	TR204	91.	cntrlvar 204	97.
Average Pin Temperature at 0.25 m High (°C)	TE201, TE203, TE210, TT217	472.	cntrlvar 210	480..
Average Pin Temperature at 0.75 m High (°C)	TE118, TE212, TE214, TE216	475.	cntrlvar 211	525.
Average Pin Temperature at 1.25 m High (°C)	TE116, TE202, TE204, TE215	554.	cntrlvar 212	560.
Average Pin Temperature at 1.75 m High (°C)	TE117, TE211, TE213, TE218	599.	cntrlvar 213	602.
Hot Pin Temp. at 0.75 m High (°C)	TE310	576.	cntrlvar 215	578.
Hot Pin Temp. at 1.25 m High (°C)	TE304	649.	cntrlvar 216	612.
Hot Pin Temp. at 1.75 m High (°C)	TE301	647.	cntrlvar 217	653.

Table 4.6 – Low Pressure Steady State nr 1 Experiment-Calculation Comparison

Controlled parameter	Experimental Value		RELAP5 boundary condition	
Loop Pressure (bar)	18.		18.	
TS Electrical Power (kW)	41.		41.	
Loop Mass Flowrate (kg/s)	0.082		0.082	
Max TS Helium Inlet Temperature	300.		300.	
Air Cooler Outlet Temperature	43.		43.	
Calculated Parameter	**HE-FUS3 Tag**	**Experimental Value**	**RELAP Reference**	**Calculated Value**
Total Pressure Drop (bar)	PD201	1.13	cntrlvar 40	1.09
TS Pressure Drop (bar)	PD229	0.364	cntrlvar 41	0.374
Valve F234 % Opening	ZT234	0.	vlvarea 172	0.
E214 Inlet Cold Side Temperature (°C)	TR215	77.	cntrlvar 215	76.
E214 Out Cold Side Temperature (°C)	TR216	300.	cntrlvar 216	318.5
E219/1 Outlet Temperature (°C)	TR223-TR236	289. -289.	cntrlvar 223	301.5
TS Outlet Temperature	TE102	377.	cntrlvar225	388.
E214 Inlet Hot Side Temperature (°C)	TR217	371.	cntrlvar 217	384.5
E214 Outlet Hot Side Temperature (°C)	TR218-TR239	141. – 141.	cntrlvar 218	131.5
Compressor Outlet Temperature (°C)	TR204	77.	cntrlvar 204	79.5
Average Pin Temperature at 0.25 m High (°C)	TE201, TE203, TE210, TE217	371.	cntrlvar 210	390..
Average Pin Temperature at 0.75 m High (°C)	TE118, TE212, TE214, TE216	387.	cntrlvar 211	415.
Average Pin Temperature at 1.25 m High (°C)	TE116, TE202, TE204, TE215	424.	cntrlvar 212	434.
Average Pin Temperature at 1.75 m High (°C)	TE117, TE211, TE213, TE218	449.	cntrlvar 213	457.
Hot Pin Temp. at 0.75 m High (°C)	TE310	451.	cntrlvar 215	471.
Hot Pin Temp. at 1.25 m High (°C)	TE304	495.	cntrlvar 216	490.
Hot Pin Temp. at 1.75 m High (°C)	TE301	506.	cntrlvar 217	512.

Table 4.7 – Low Pressure Steady State nr 2 Experiment-Calculation Comparison

	Experiment	Calculation
First step start-up	0,78	0,9
Second step start-up	0.78	0.76
Third step start-up	0.83	0.83
Forth step start-up	0.88	0.89
Additional step start-up	0.85	0.9
Low pressure steady state 1	0.90	0.96
Low pressure steady state 2	0.77	0.81

Table 4.8 –Experimental and Calculated Heat Losses in the different SS conditions

Heat Losses (kW)	Experimental (Estimated)	Post-test calculations
First step start-up	14.9	15,1
Second step start-up	15.2	16.1
Third step start-up	23.	21.8
Forth step start-up	26.1	23.8
Additional step start-up	25.2	25.2
Low pressure steady state 1	23.7	25.2
Low pressure steady state 2	15	18.9

Table 4.9 – Economizer Efficiency in the different SS conditions

4.3 LOFA through Compressor Speed Reduction

As described in § 2.2 the first LOFA transient followed the reduction of compressor speed. The results of the post-test calculation for the main measured parameters are reported in Figs. 4.1 to 4.11 in comparison with the experimental data. Due to the insufficiency of the compressor model the correspondent mass flowrate decreasing (Fig. 4.1) as well as the increasing that followed the restore of the initial speed has been directly imposed.

Due to the decease of the mass flowrate the temperatures increase in the hot part of the loop, as a consequence the by-pass valve 234 has operated to maintain the temperature at 300 °C at the inlet of the test section. The initial value of the valve opening in Fig. 4.2 is slightly over estimated as the characteristic of the valve has not been calibrated on the experimental data, moreover the operation is slightly anticipated in the calculation.

The inlet and outlet economizer temperatures in Figs. 4.4 and 4.5 explain the reason for this discrepancy between calculation and experiment. For instance the temperature TR 216 at the

outlet of the economizer cold side, which gives the main indication of the loop heating up, is not comparable with the calculated helium temperature (cntrlvar 201) because it is strongly influenced by the thermal capacity of the wall. In fact, its trend is very similar to those of the temperature calculated within the first layer of the wall (cntrlvar 231). This situation is common to all measured helium temperatures a part from the new thermocouples implemented in the Test Section and will have to be taken into account in the future experimental activity as well as in the upgrading of the model.

Figure 4.5 shows also that the temperature increase is higher in the calculation but this result was expected because the decrease of mass flowrate causes a decrease of the economizer efficiency that is not correctly simulated by the numerical model, as already stated commenting on the steady state results.

Thanks to the control of the temperature at the inlet of the Test Section the calculated trend of the helium temperature at the TS outlet is in good agreement with the experimental one (Fig. 4.6).

The cladding temperature calculated for the average pin at the different elevations (Fig. 4.6 to 4.9) is bounded by the experimental temperatures (only 4 thermocouples of 6 are considered reliable) except for the position at 0.75 m (Fig. 4.7) where the calculated value is 50 °C higher. Even considering the uncertainty on the helium temperature and heat transfer coefficient there is not explanation for such a difference, that therefore would require a further investigation on the position and installation of the thermocouples on the pins. At the higher elevation the trend of the experimental temperatures during the transient show a deterioration of the heat transfer performance with the increase of the helium temperature that is not reproduced by the numerical model.

Similar observations are also valid for the cladding temperature in the hot pin (Fig. 4.11). In this case the measurements are available at only three elevations (0.75, 1.25 and 1.75), moreover the thermocouple at 1.25 m gives a too higher value that does not seem reliable. At the remaining elevations the calculation values are in very good agreement with the experimental ones during all the transient.

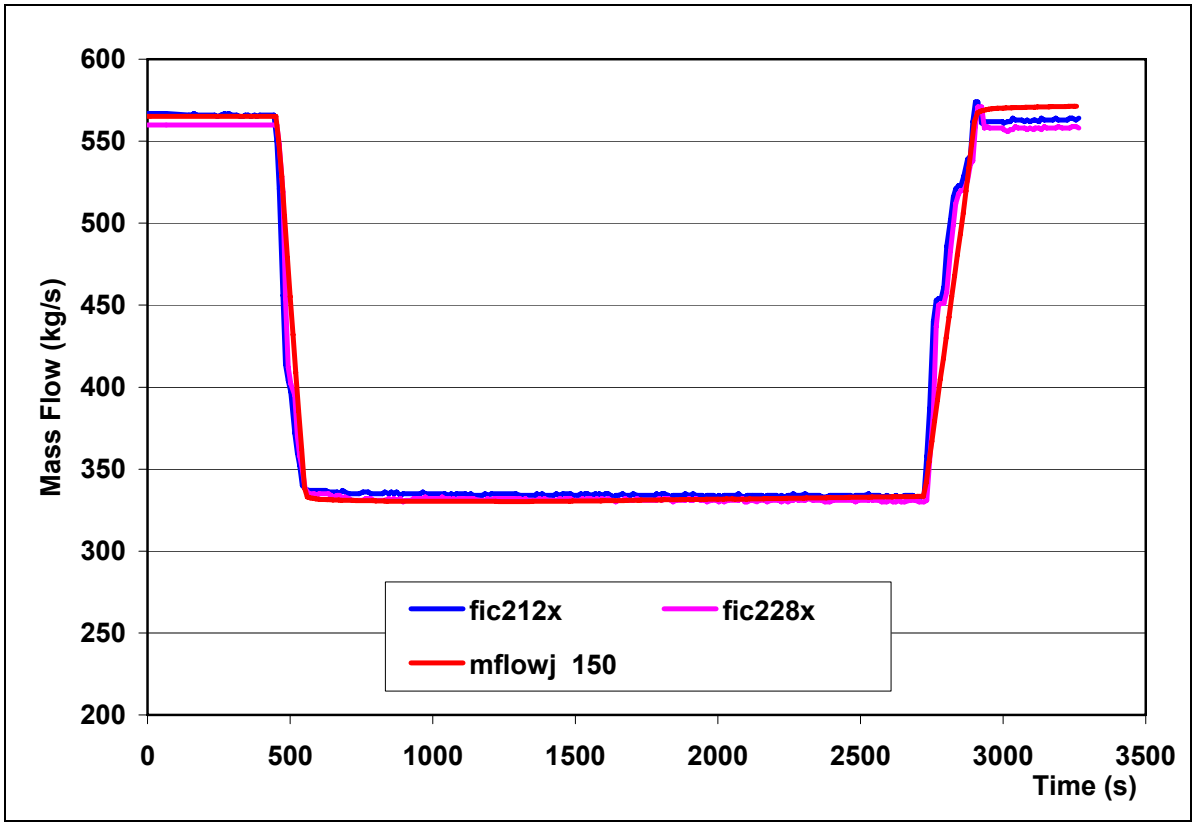

Fig.4.1 – Compressor and Test Section Mass Flow

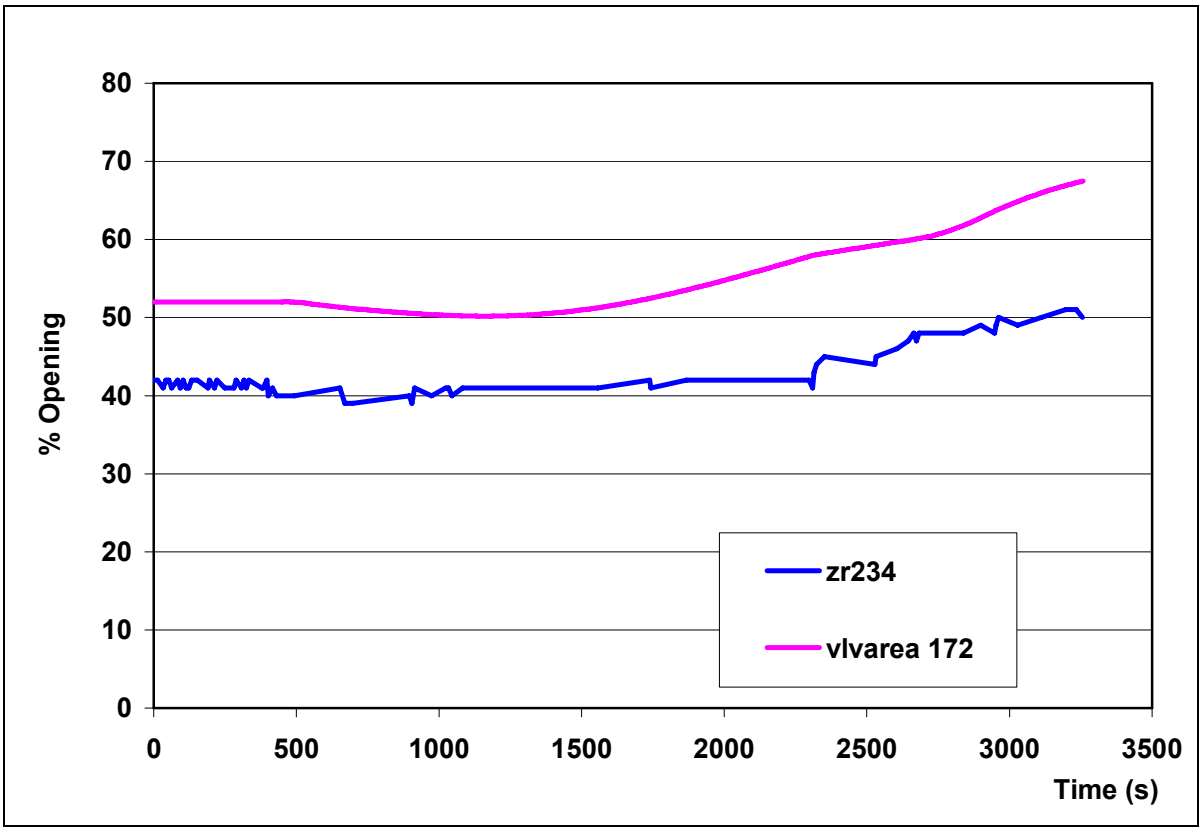

Fig.4. 2 – Main and Bypass Valves Opening

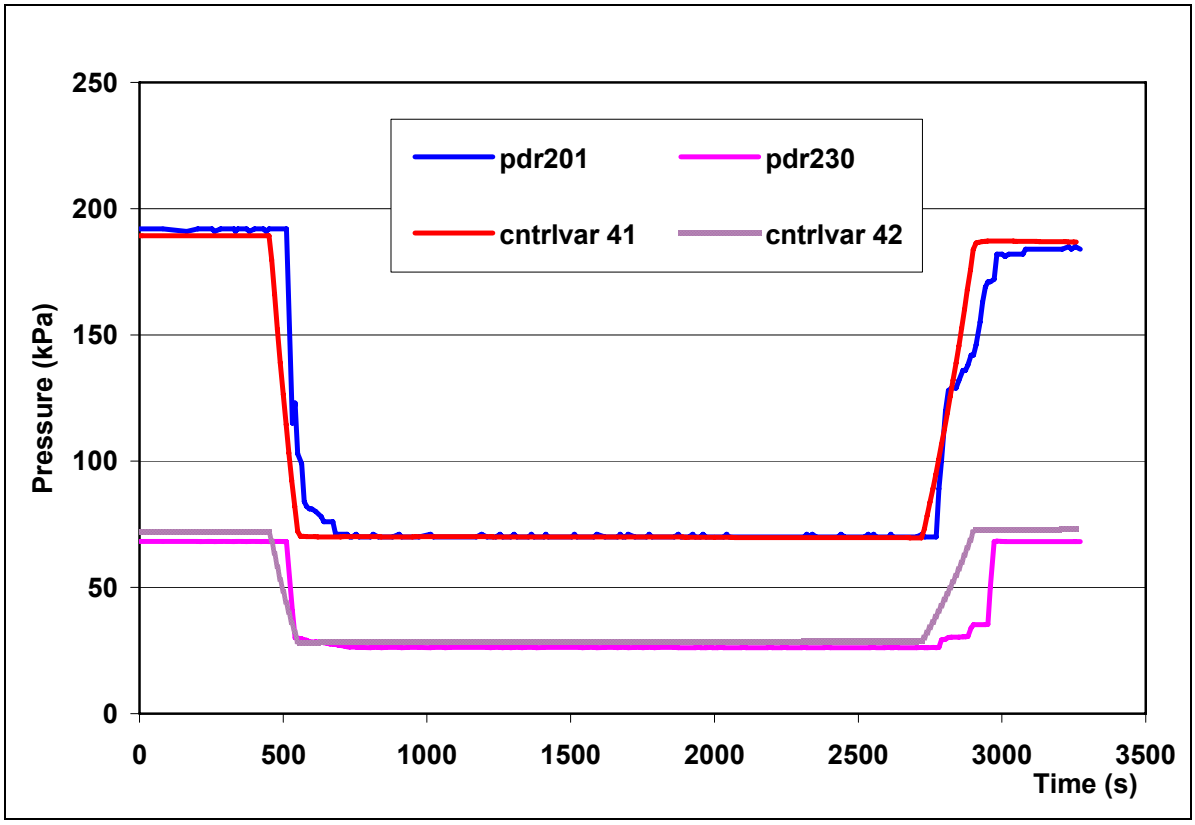

Fig. 4.3 – Loop and Test Section Pressure Drops

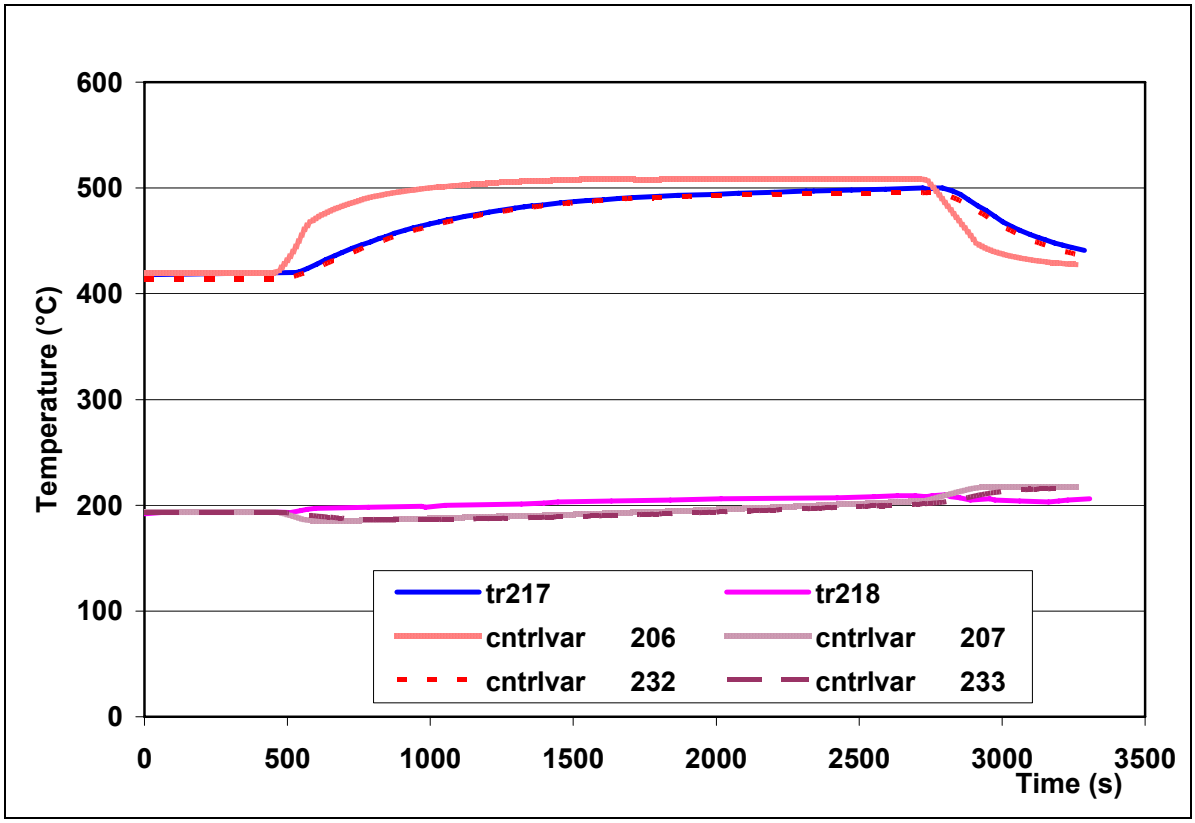

Fig. 4.4 – In and Out Economizer Hot Side Temperatures

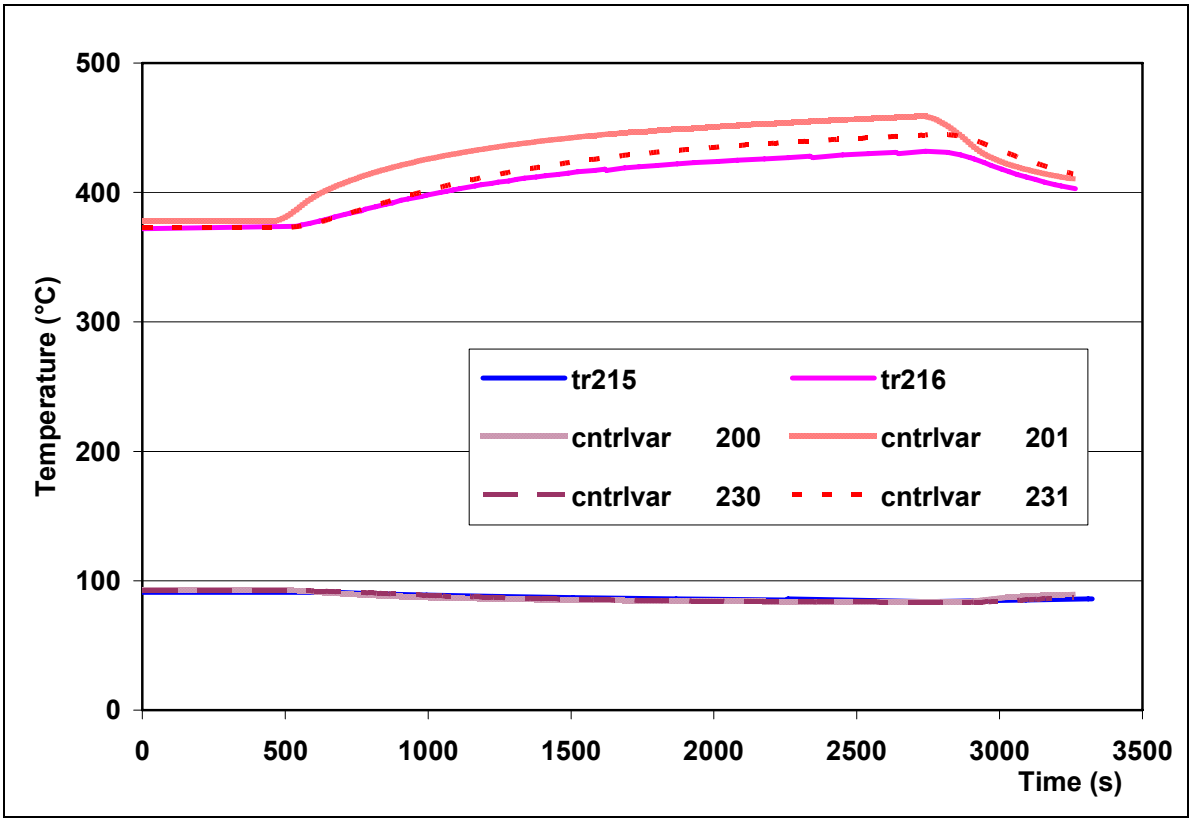

Fig. 4.5 – In and Out Economizer Cold Side Temperatures

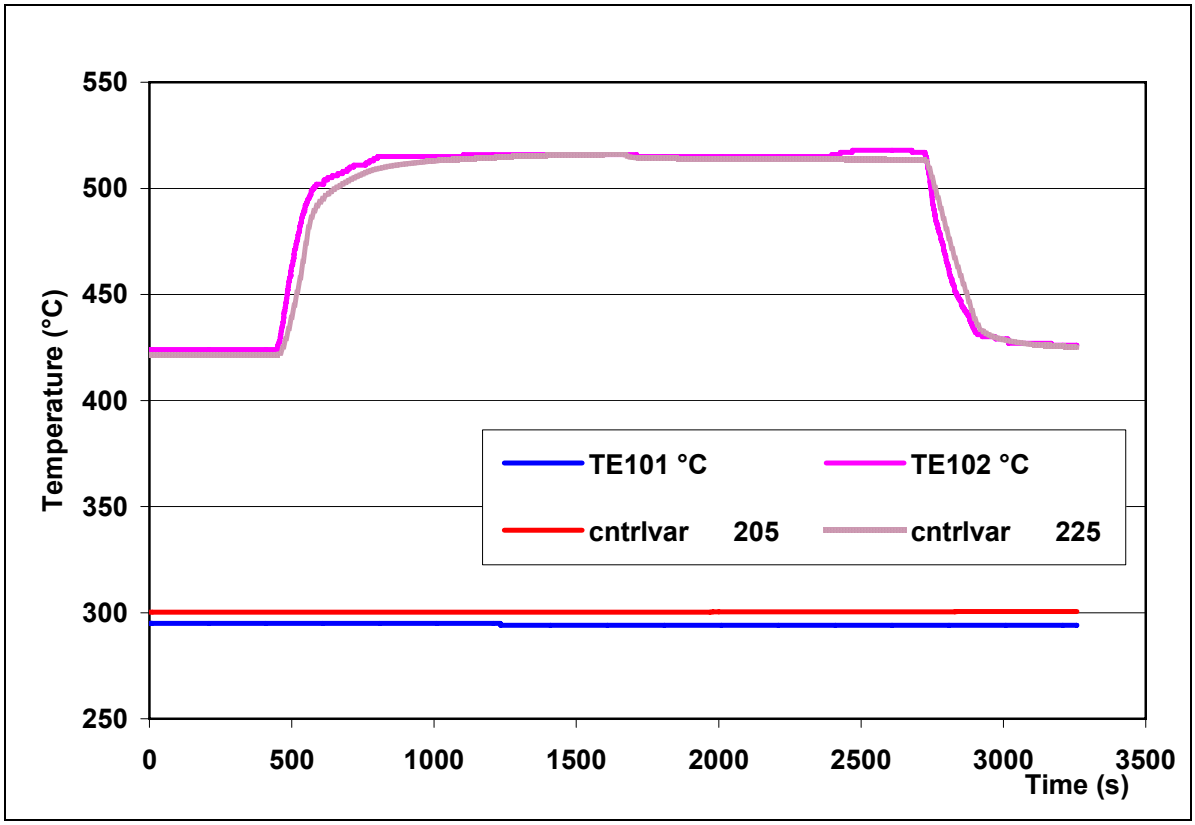

Fig. 4.6 – Inlet and Outlet TS Temperatures

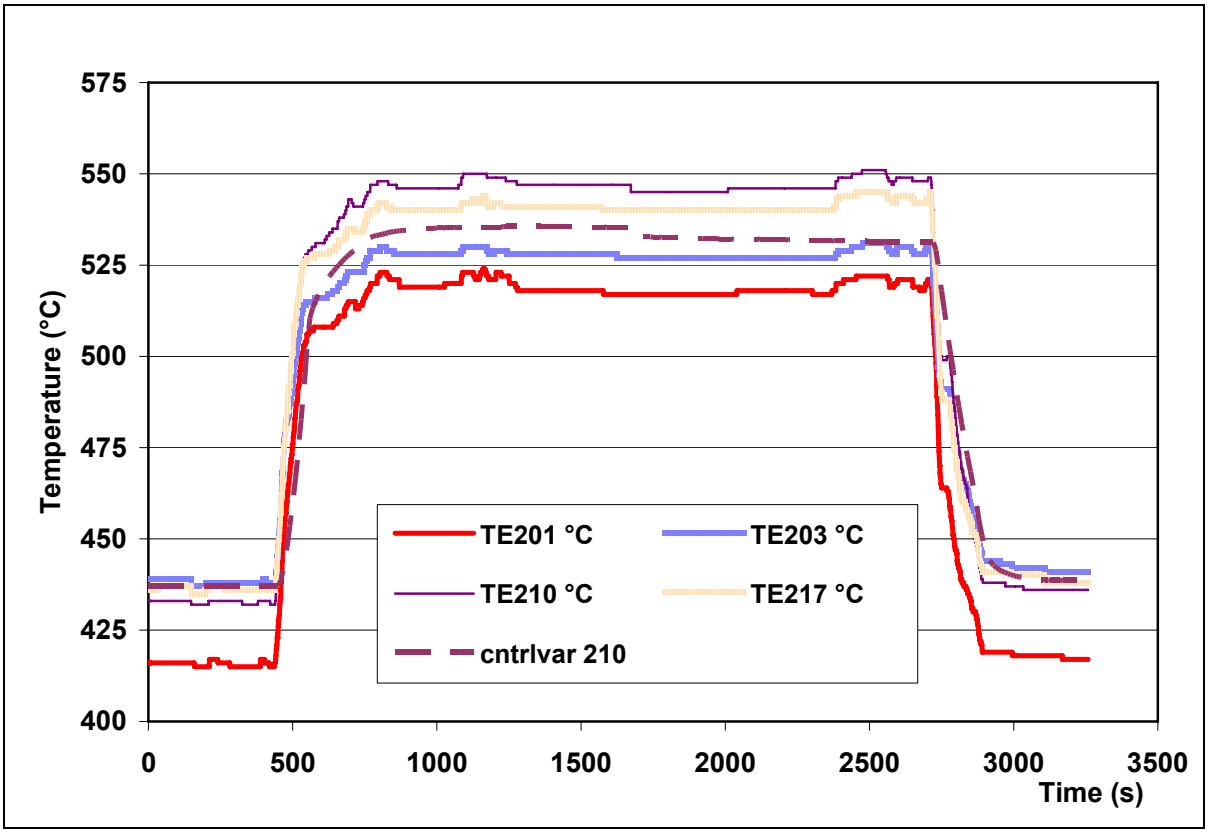

Fig. 4.7 – Pins 1-6 average temperature at 0.25 m

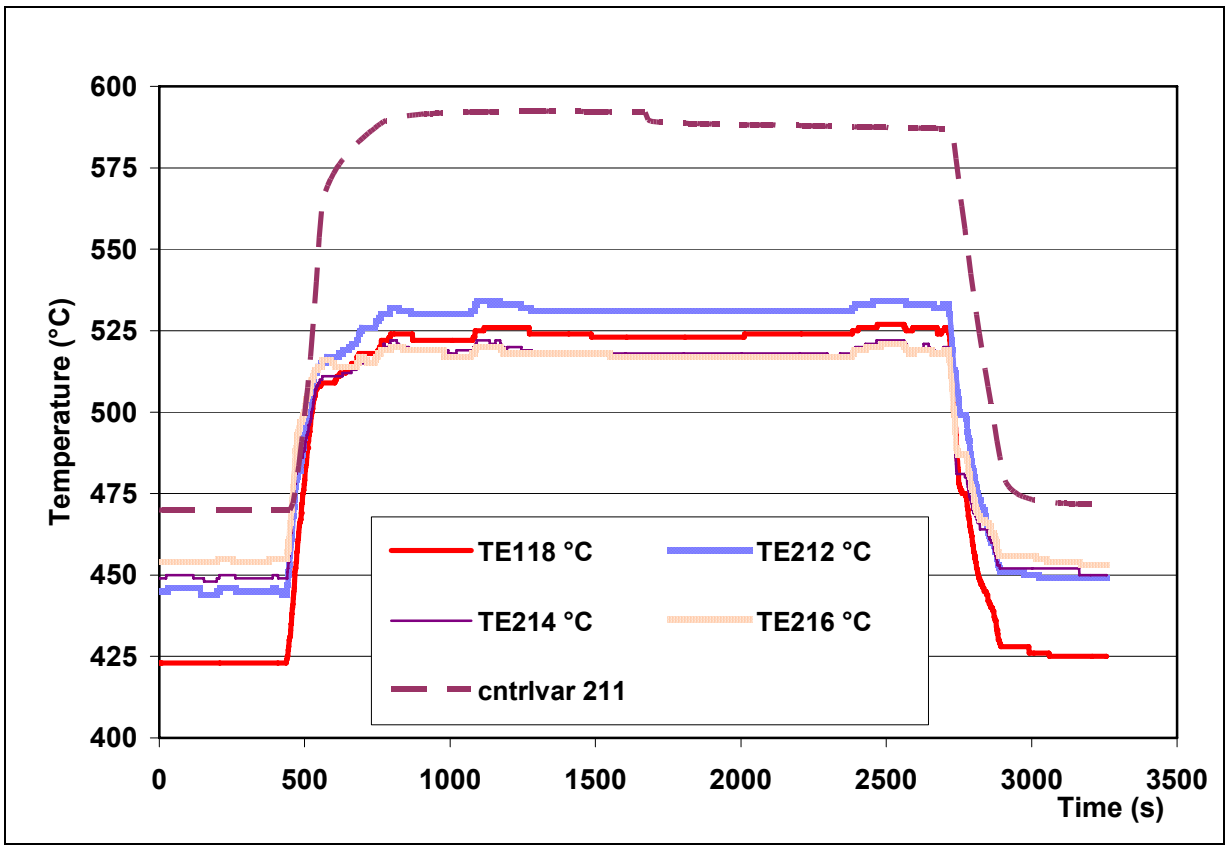

. Fig. 4.8 – Pins 1-6 average temperature at 0.75 m

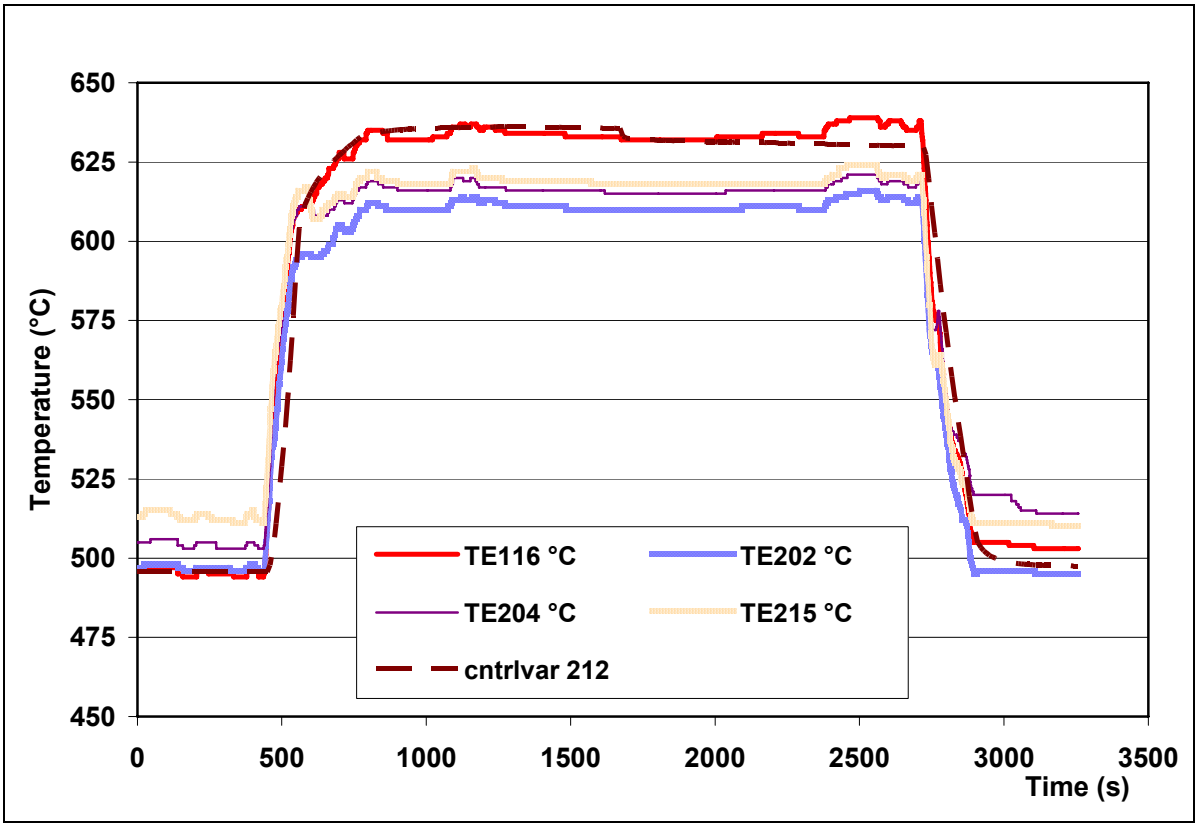

. Fig. 4.9 – Pins 1-6 average temperature at 1.25 m

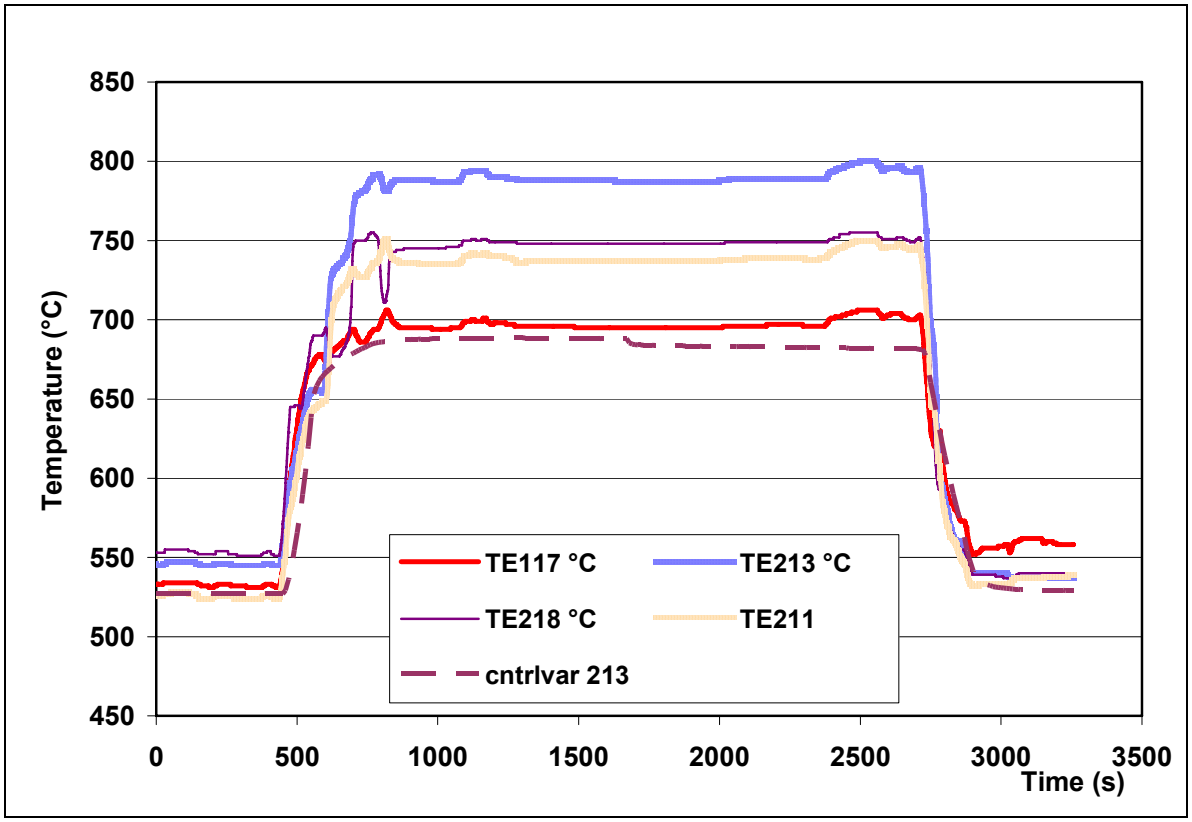

. Fig. 4.10 – Pins 1-6 temperatures at 1.75 m

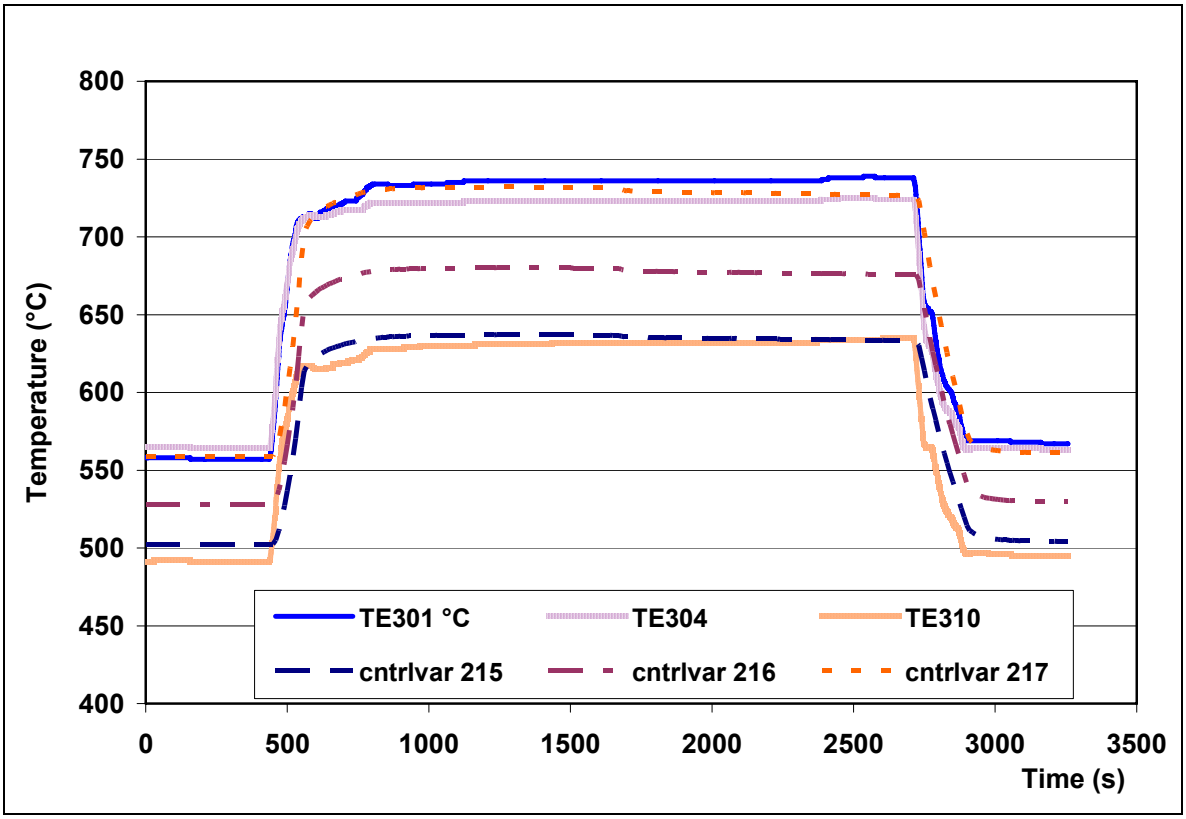

. **Fig. 4.11 – Pins 7 temperature at 0.75, 1.25 and 1.75 m**

4.3 LOFA Transient through By-pass Valve Opening

The second LOFA transient was started off by the complete opening of the valve F235 and ended by closing again the valve according the timing reported in § 2.2. The results of the post-test calculation for the main measured parameters are reported in Figs. 4.12 to 4.22 in comparison with the experimental data.

The opening of an alternative flow path causes the decrease of the mass flowrate through the economizer and consequently the increase of temperatures in the hot part of the loop and in the test section. On the contrary, due to the decrease of the total hydraulic resistance of the loop the compressor mass flowrate increases as showed in Fig. 4.12. RELAP5 calculation shows a slight overestimation of the mass flowrate in the test section, while this overestimation, which is directly connected to the compressor model insufficiency, is more evident through the compressor itself. Besides the need to improve the compressor model already discussed in § 4.1 the trend of the loop pressure drop in Fig. 4.14 suggests to re-calibrate the valve characteristic adopted in the numerical model against the experimental data.

The operation of the by-pass valve 234 (Fig. 4.13) is qualitatively well reproduced, the discrepancies between calculation and experiment are still explained by the discussed in the previous paragraph.

In the inlet and outlet economizer temperatures in Figs. 4.15 and 4.16 the influence of the thermal wall capacity remarked previously is evident. In fact, the experimental temperature trends are in very good agreement with the temperatures calculated within the first layer of the pipe walls rather then the helium temperatures. Respect to the previous LOFA the economizer efficiency seems not influenced by the variation of the flow conditions and results correctly simulated during all the transient.

In spite of the control of the TS inlet temperature, the outlet temperature in Fig. 4.17 is slightly underestimated during the transient because of the overestimation of the mass flowrate.

The previous discussion on the pin cladding temperatures (Figs. 4.18 to 4.22) is still valid for this transient, just it has to be noticed that at the higher elevation the thermocouples on the pins 6 and 5 present a sharp drop in the temperatures due to an approach of the pins themselves. At the higher elevation both the normal pins and the hot pin show a deterioration of the heat transfer performance with the increase of the helium temperature that is not reproduced by the numerical model.

Similar observations are also valid for the cladding temperature in the hot pin (Fig. 4.11). In this case the measurements are available at only three elevations (0.75, 1.25 and 1.75), moreover the thermocouple at 1.25 m gives a too higher value that does not seem reliable. At the remaining elevations the calculation values are in very good agreement with the experimental ones during all the transient.

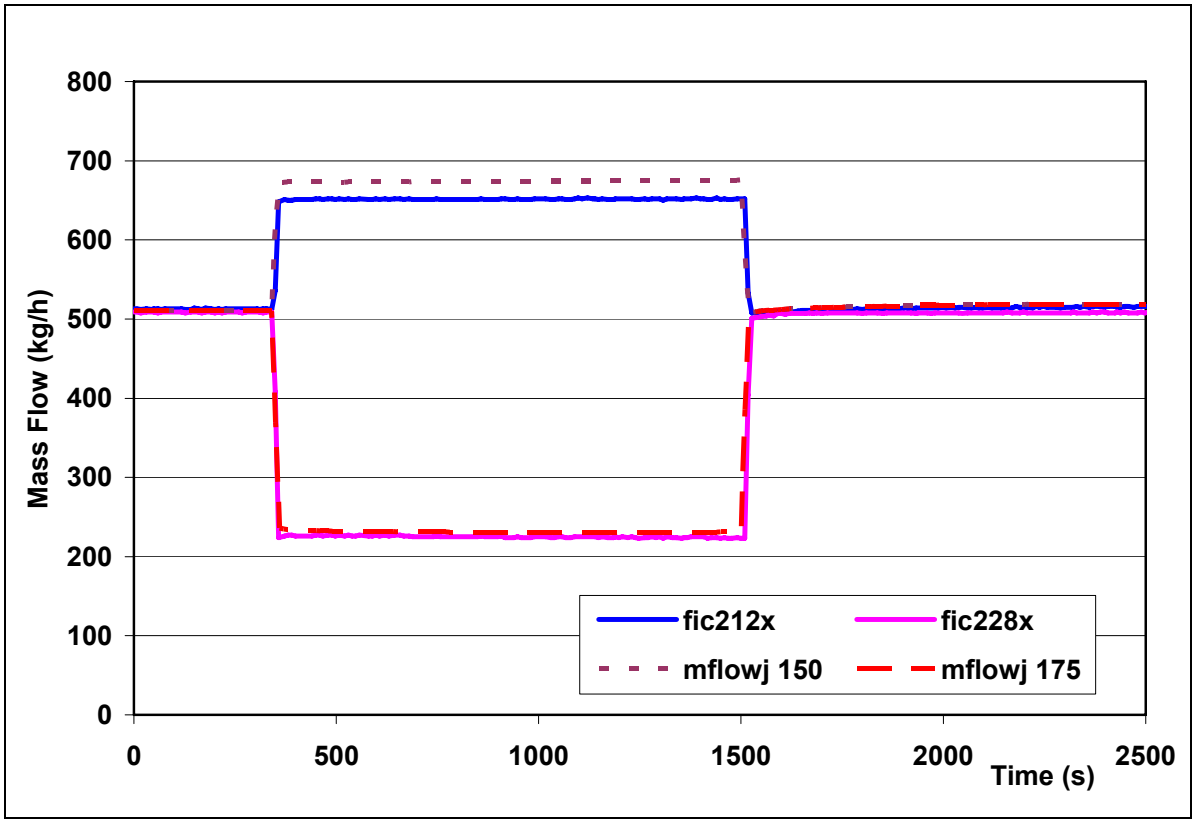

Fig.4.12 – Compressor and Test Section Mass Flow

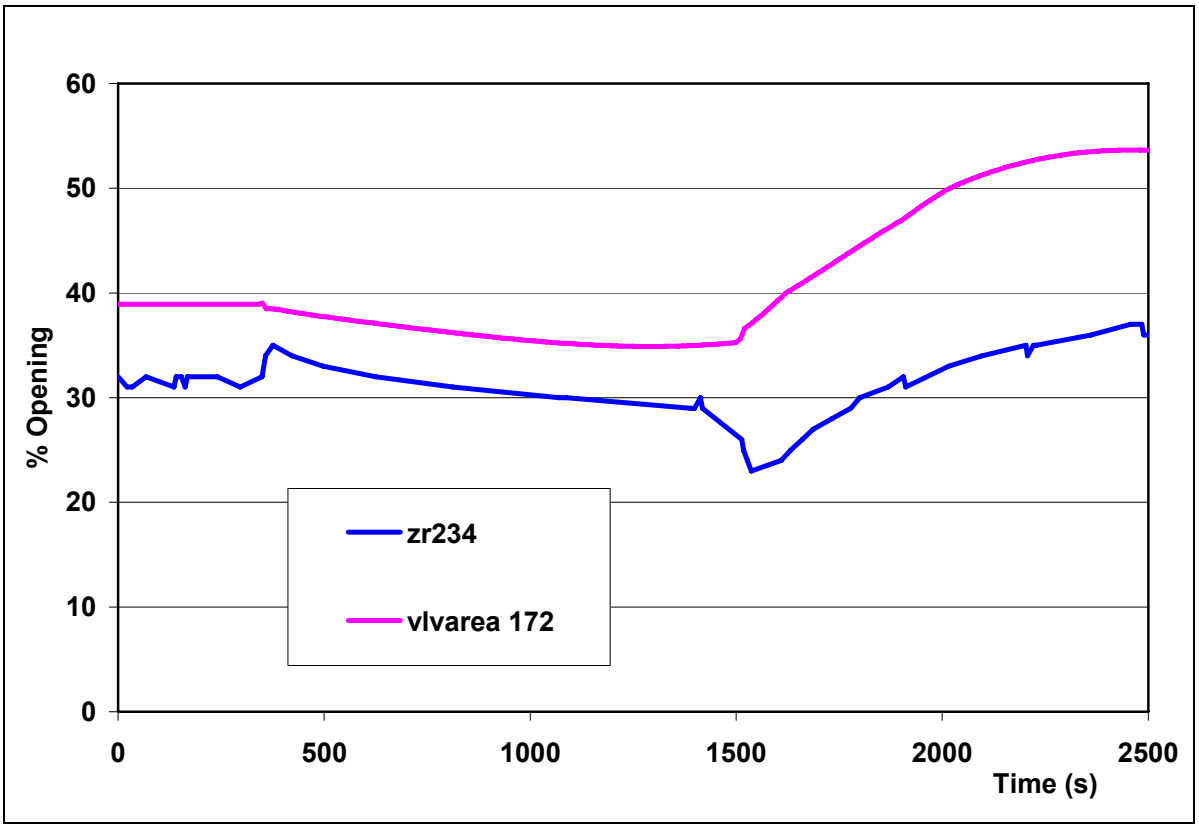

Fig.4.13 –Bypass Valves Opening

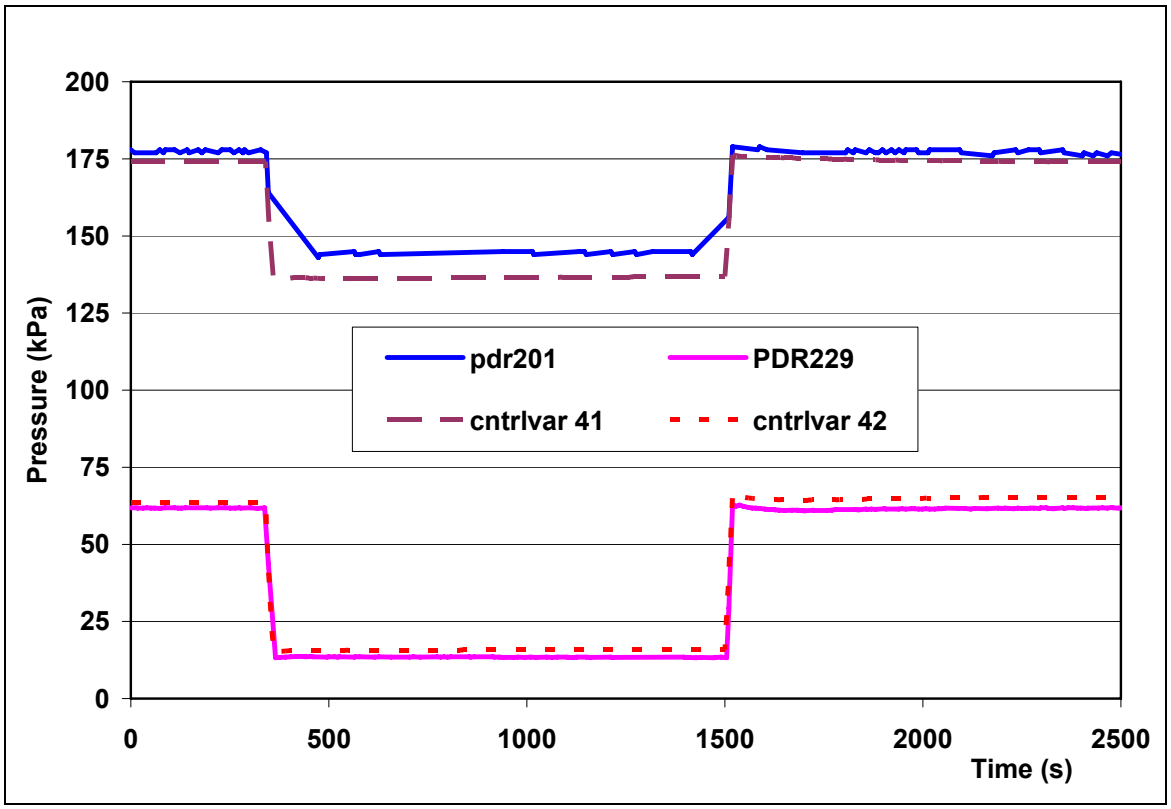

Fig. 4.14 – Loop and Test Section Pressure Drops

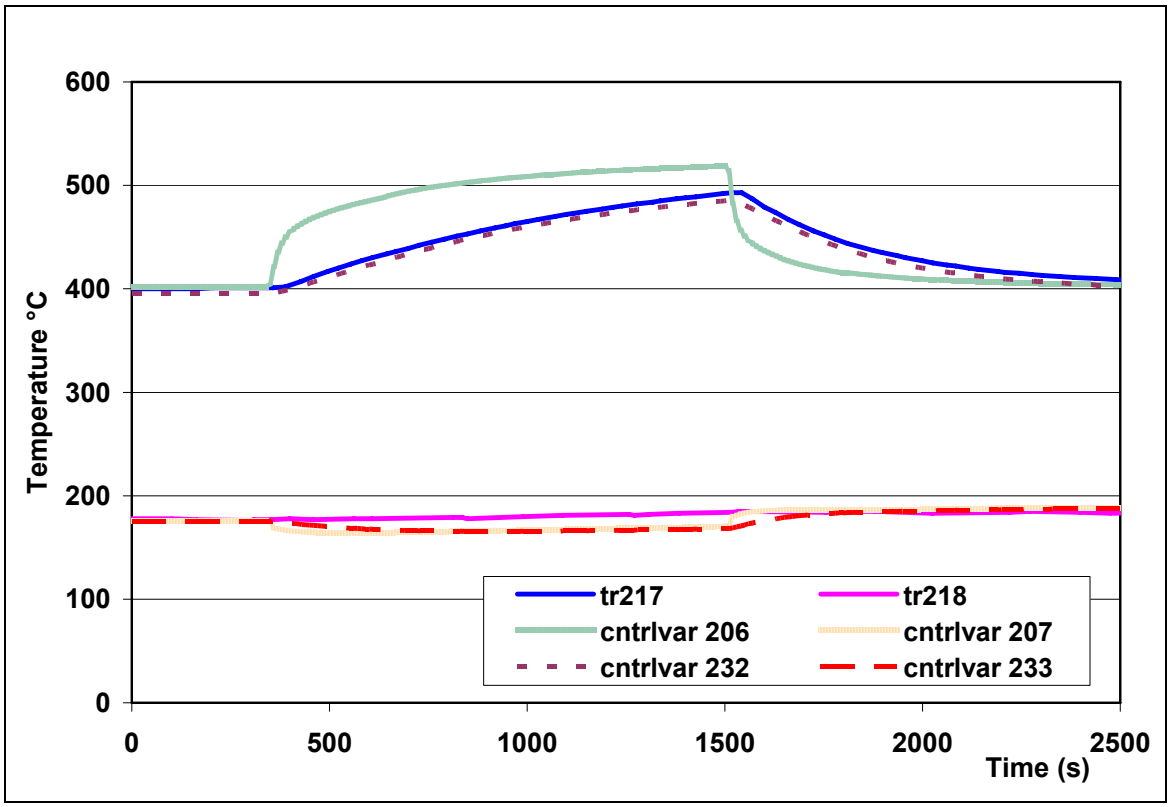

Fig. 4.15 – In and Out Economizer Hot Side Temperatures

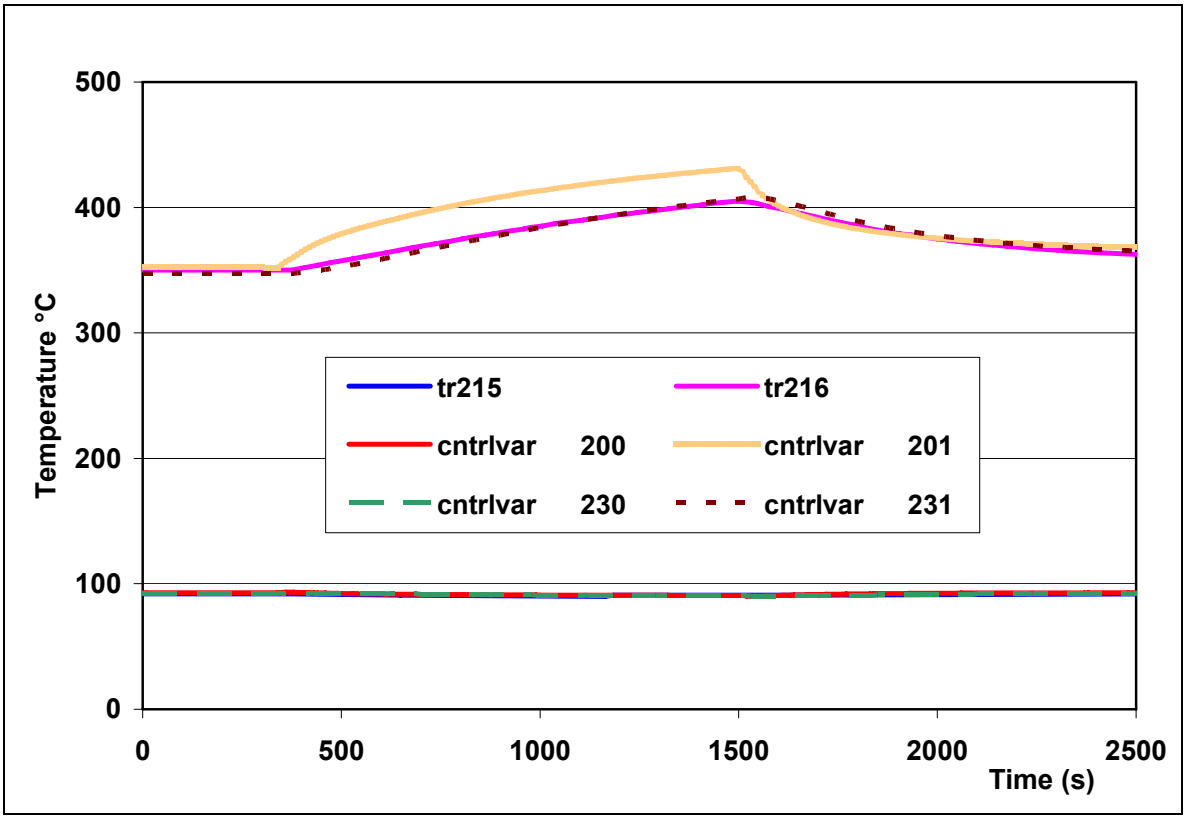

Fig. 4.16 – In and Out Economizer Cold Side Temperatures

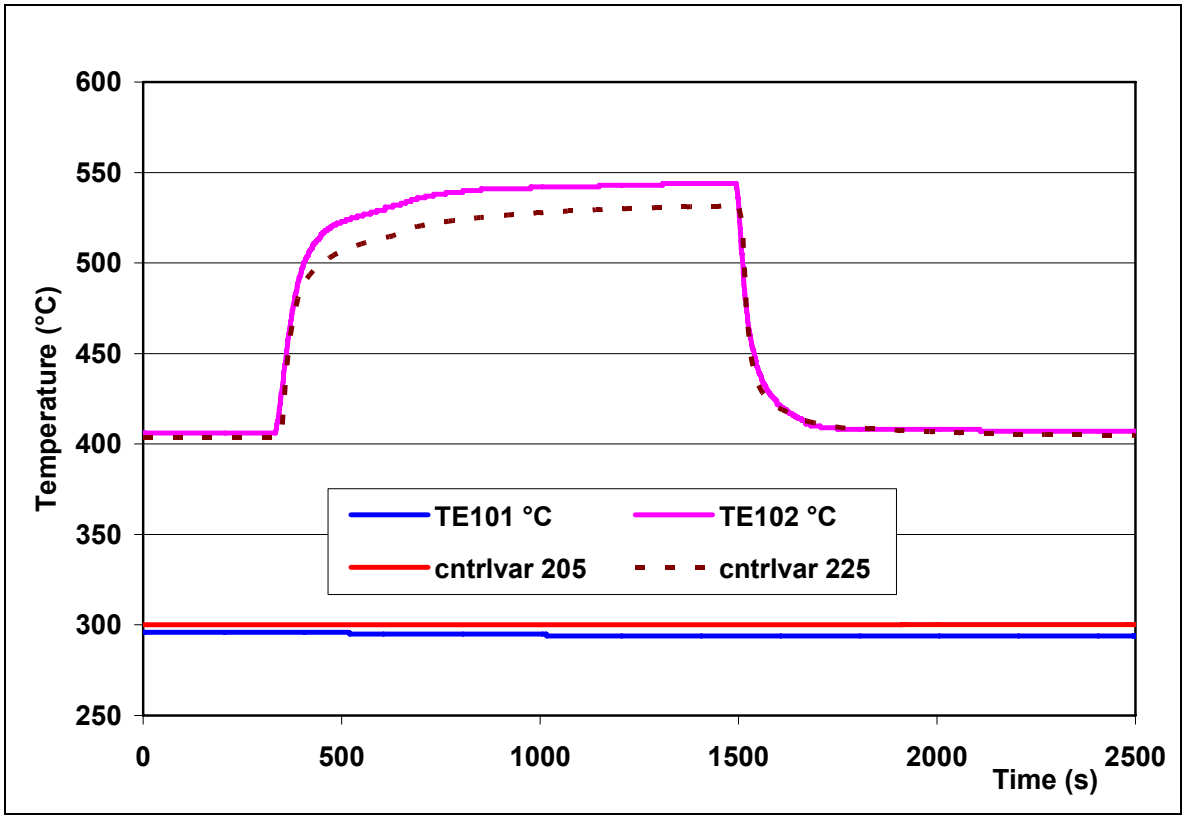

Fig. 4.17 – Inlet and Outlet TS Temperatures

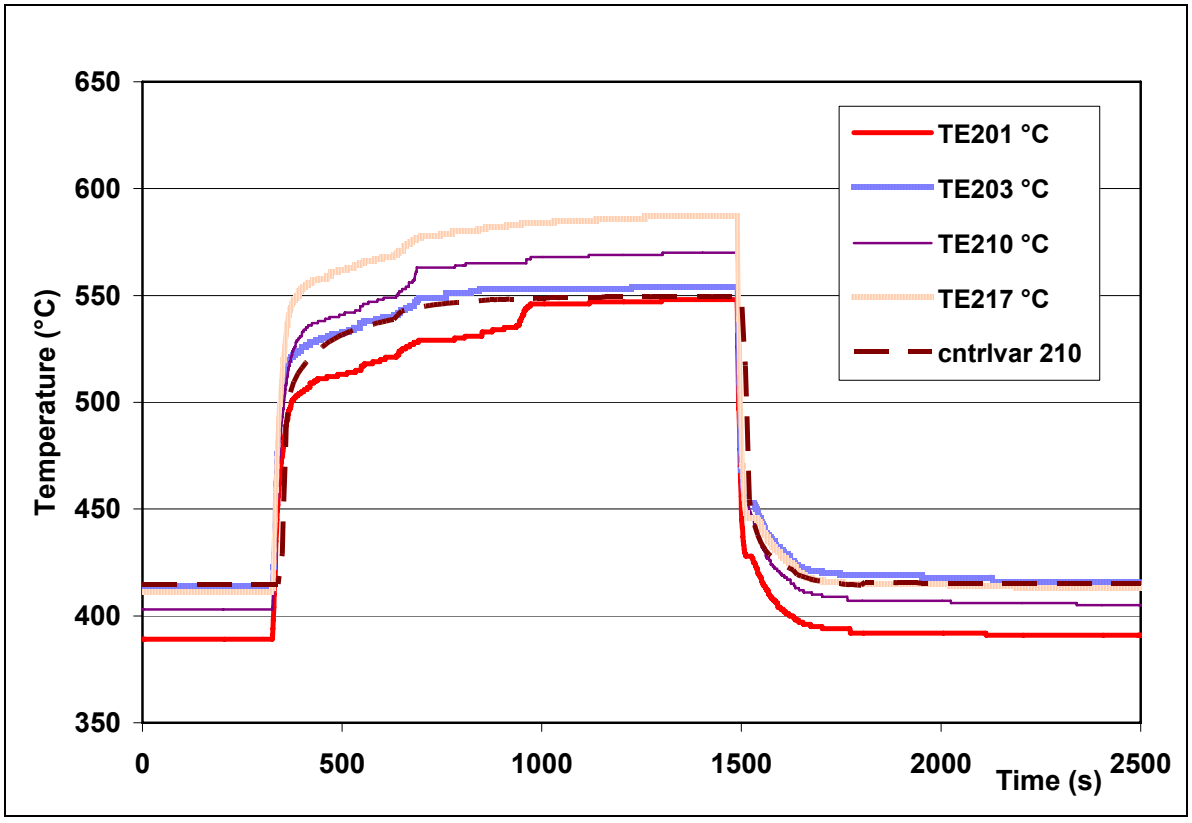

Fig. 4.18 – Pins 1-6 average temperature at 0.25 m

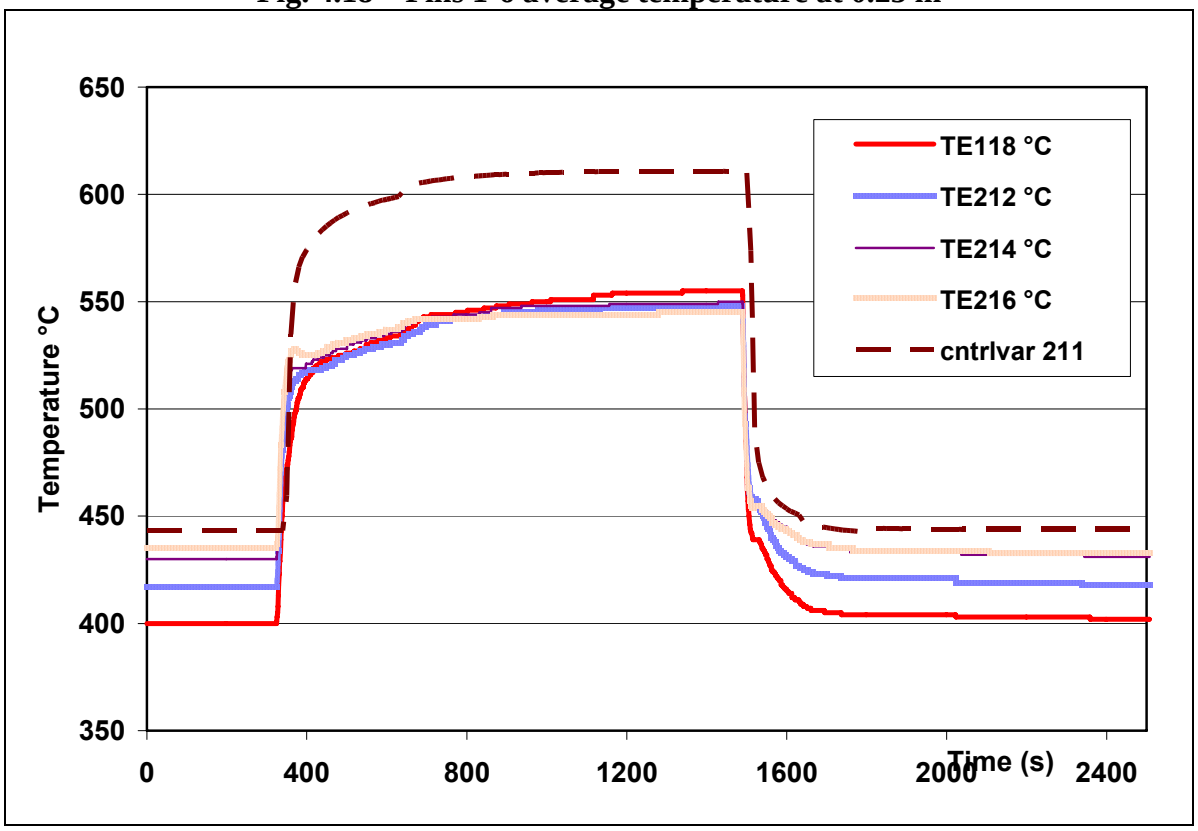

. Fig. 4.19 – Pins 1-6 average temperature at 0.75 m

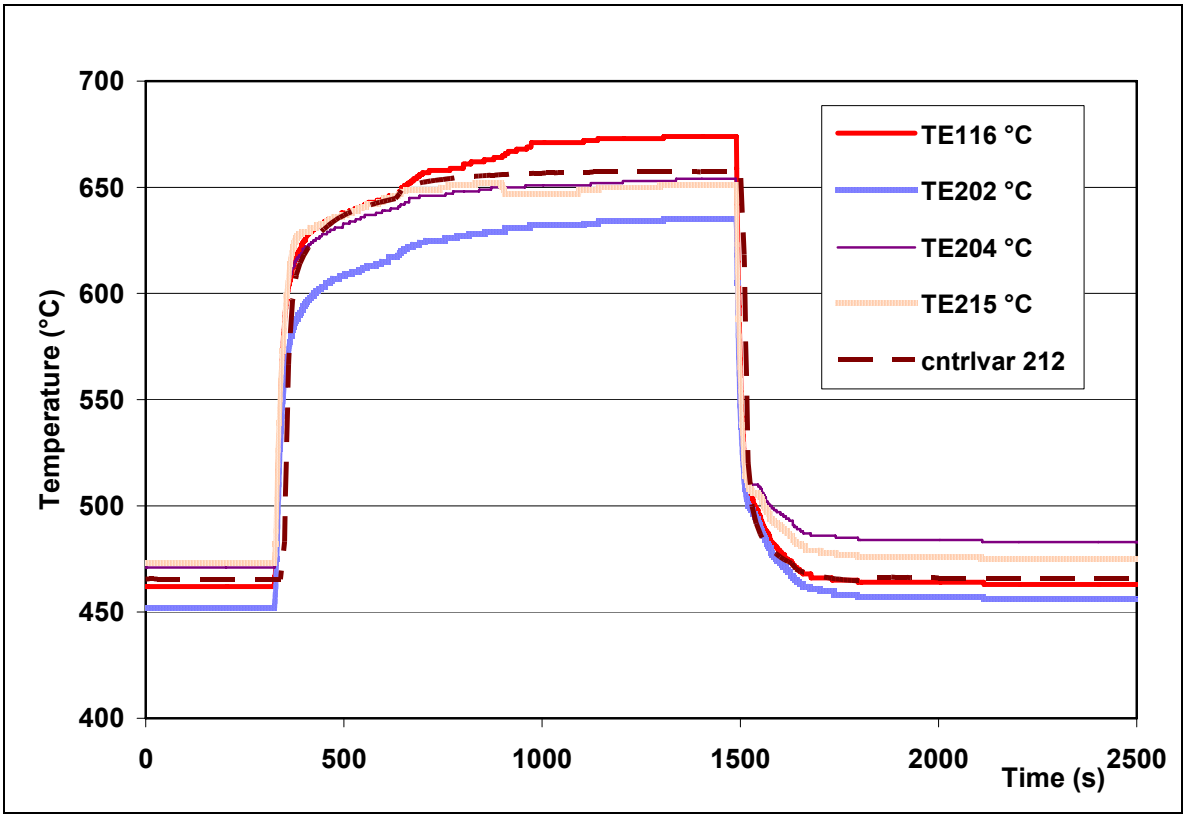

. Fig. 4.20 – Pins 1-6 average temperature at 1.25 m

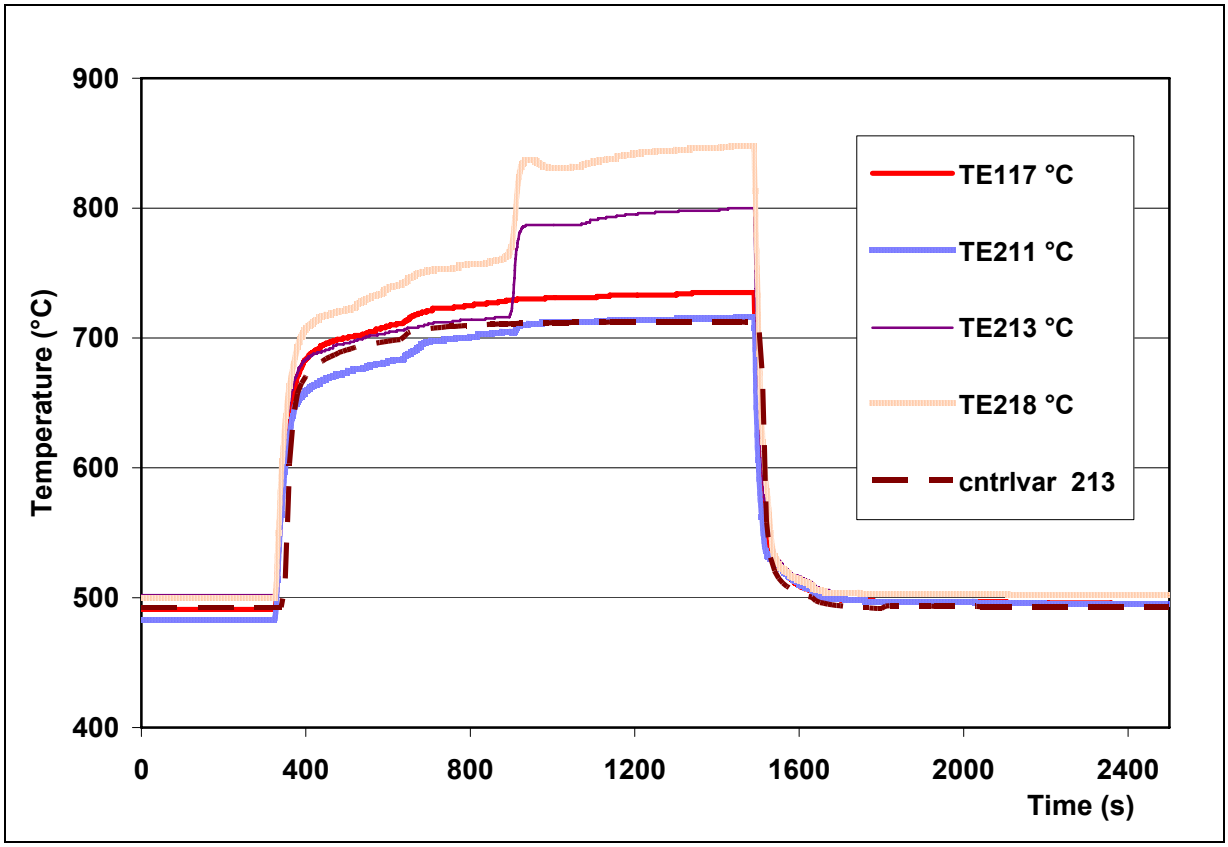

. Fig. 4.21 – Pins 1-6 average temperature at 1.75 m

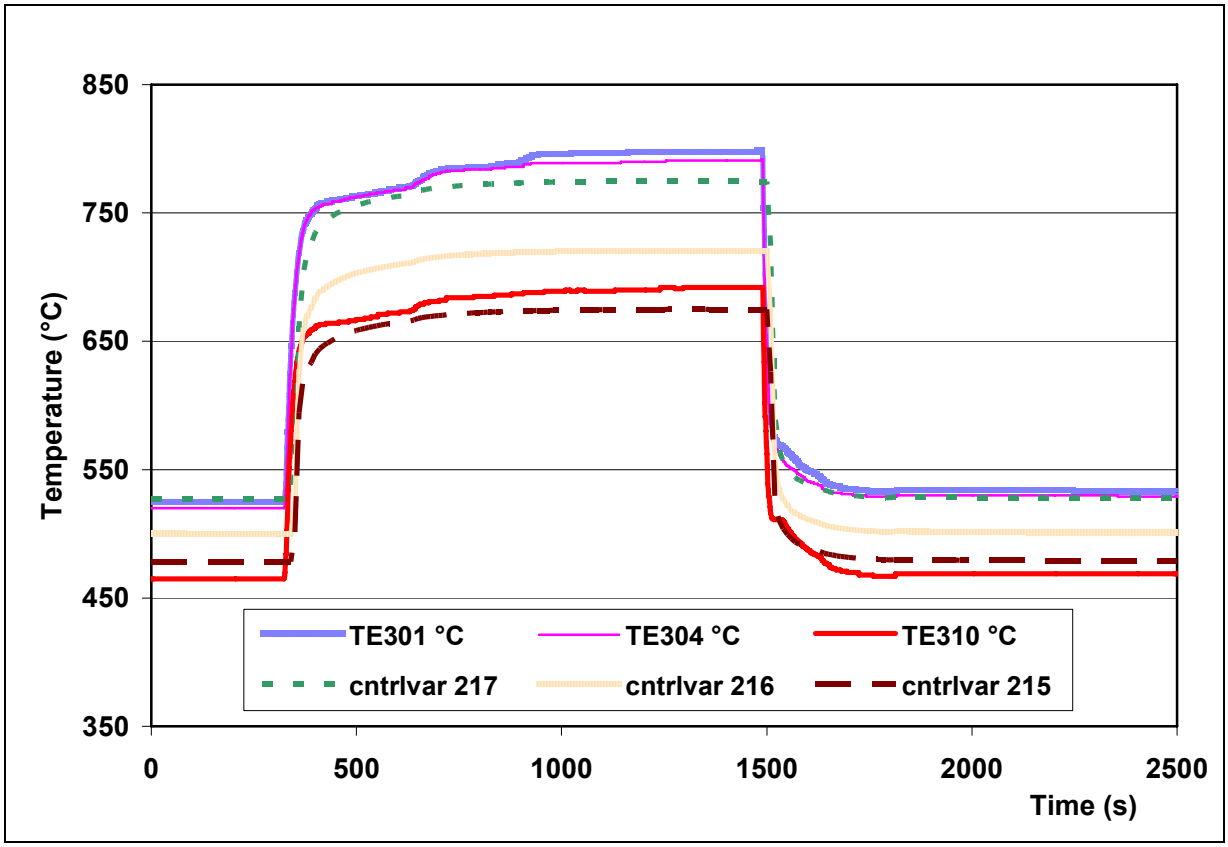

. **Fig. 4.22 – Pins 7 temperature at 0.75, 1.25 and 1.75 m**

4.3 LOCA at 30 bar

The first LOCA transient was conducted starting with a loop pressure of about 30 by opening the set of the valves available on the tank as described in § 2.3. The results of the post-test calculation for the main measured parameters are reported in Figs. 4.23 to 4.33 in comparison with the experimental data.

Due to the complex geometry of the simulated break (position of the three valves, discharge pipes dimensions and connections) the value of the break flow area in the RELAP5 model has been calibrated in order to reproduce the experimental pressure (Fig. 4.23). Unfortunately the sensitivity of the pressure measurements on the loop are really low (about 1 bar), so the uncertainty on the boundary conditions for this transient results quite high.

The relatively fast depressurization of the loop causes the sharp decrease of the helium density and consequently the decrease of the loop mass flowrate. The compressor speed is maintained constant in the simulation as in the experiment, so the compressor model is of fundamental importance for the calculation of the new mass flowrate. In 4.24 the comparison between calculated and measured mass flowrate proves that the compressor model is not able to correct reproduce the head characteristic curves varying the loop conditions, in fact, the mass flowrate is remarkably underestimated.

As a consequence of the decrease of mass flowrate, the temperatures increase in the hot part of the loop. The simulation of the by-pass valve 234 operation (Fig. 4.25) agrees with the previous results.

For the inlet and outlet economizer temperatures in Figs. 4.26 and 4.27 are still valid the observations made before, including the negative effect of the flow conditions on the economizer efficiency that is not correctly simulated during the transient.

No particular comment has to be made on the TS helium and pin temperatures (Figs. 4.28 to 4.33) because the trends are very similar to those already discussed for the LOFA transients in § 4.2 and 4.3.

.

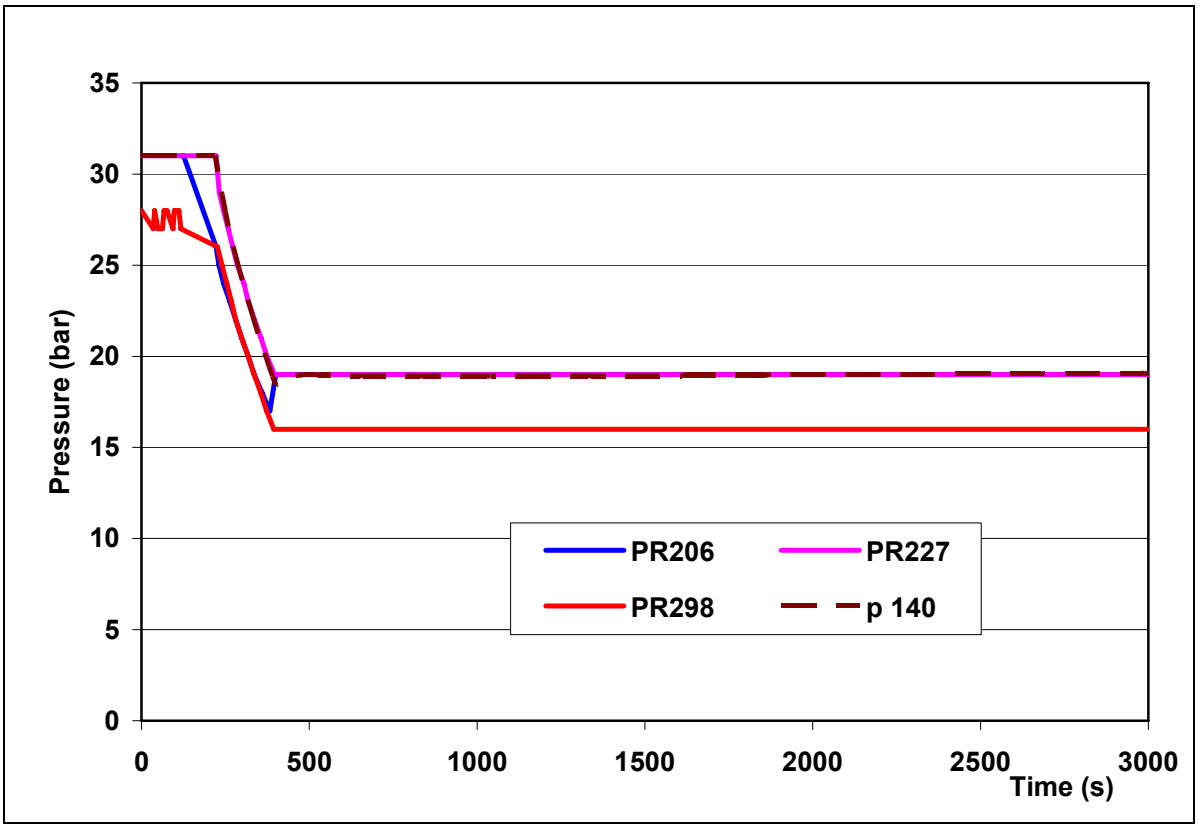

Fig.4.23 – Loop Pressures

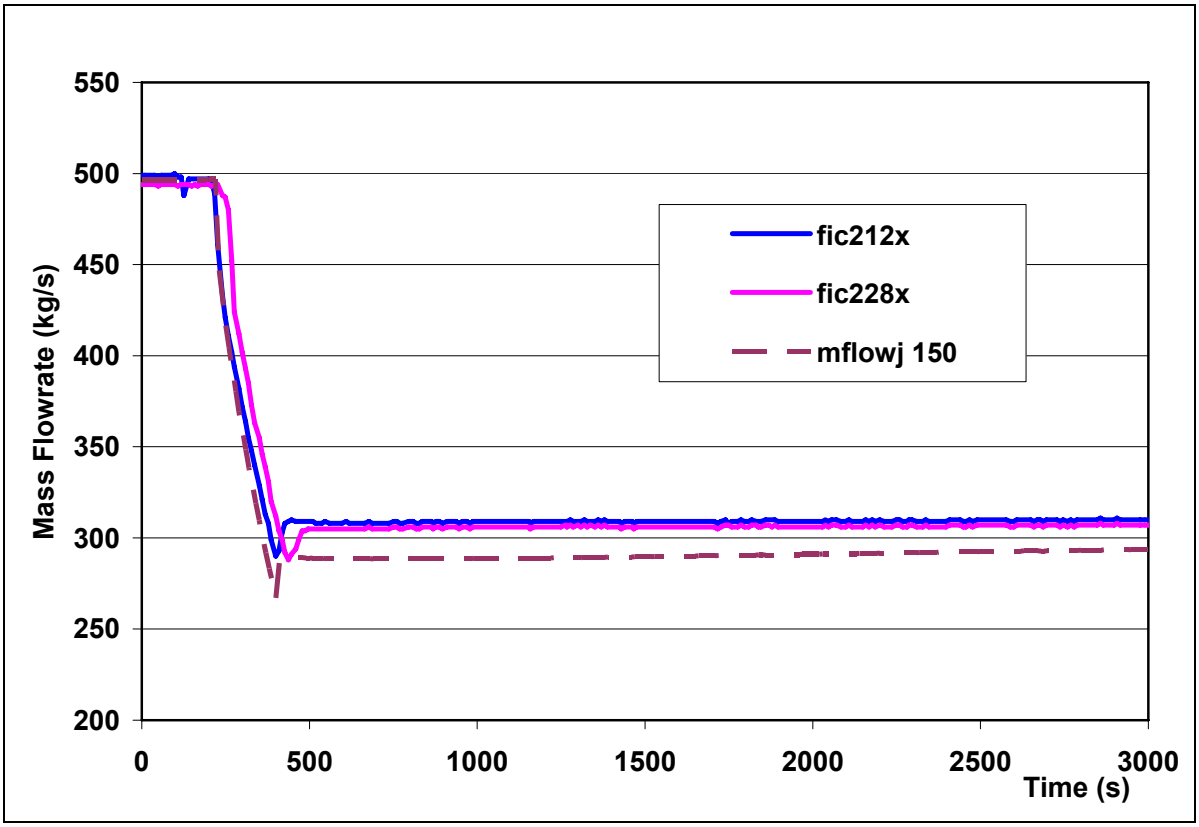

Fig. 4.24 –Loop Mass Flowrate

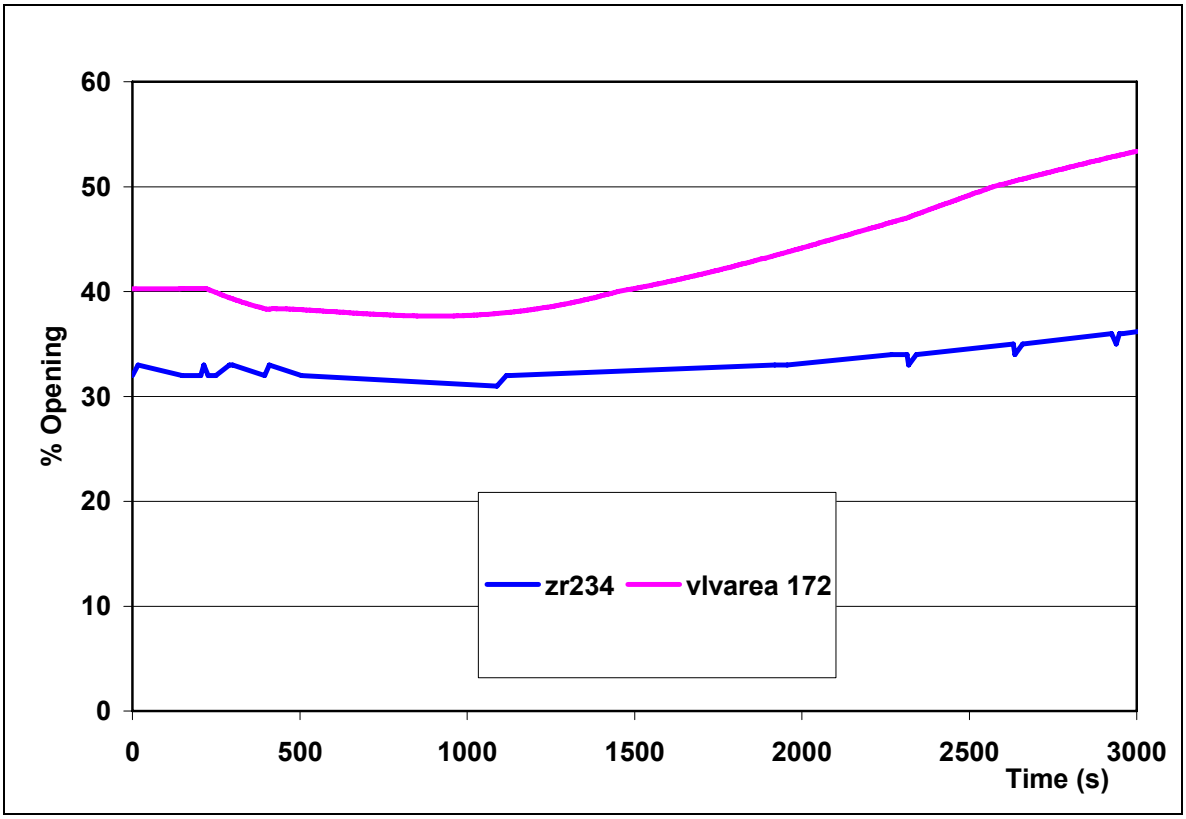

Fig.4.25 – Bypass Valves Opening

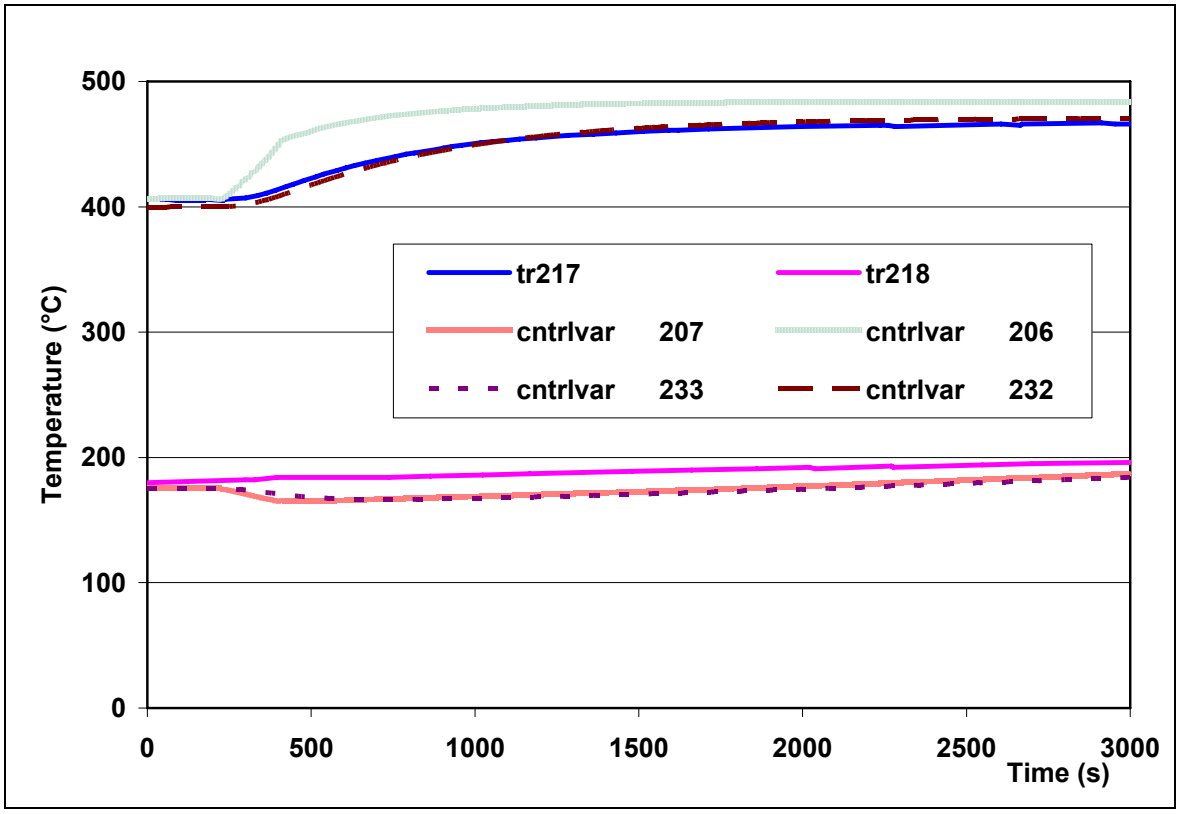

Fig. 4.26 – In and Out Economizer Hot Side Temperatures

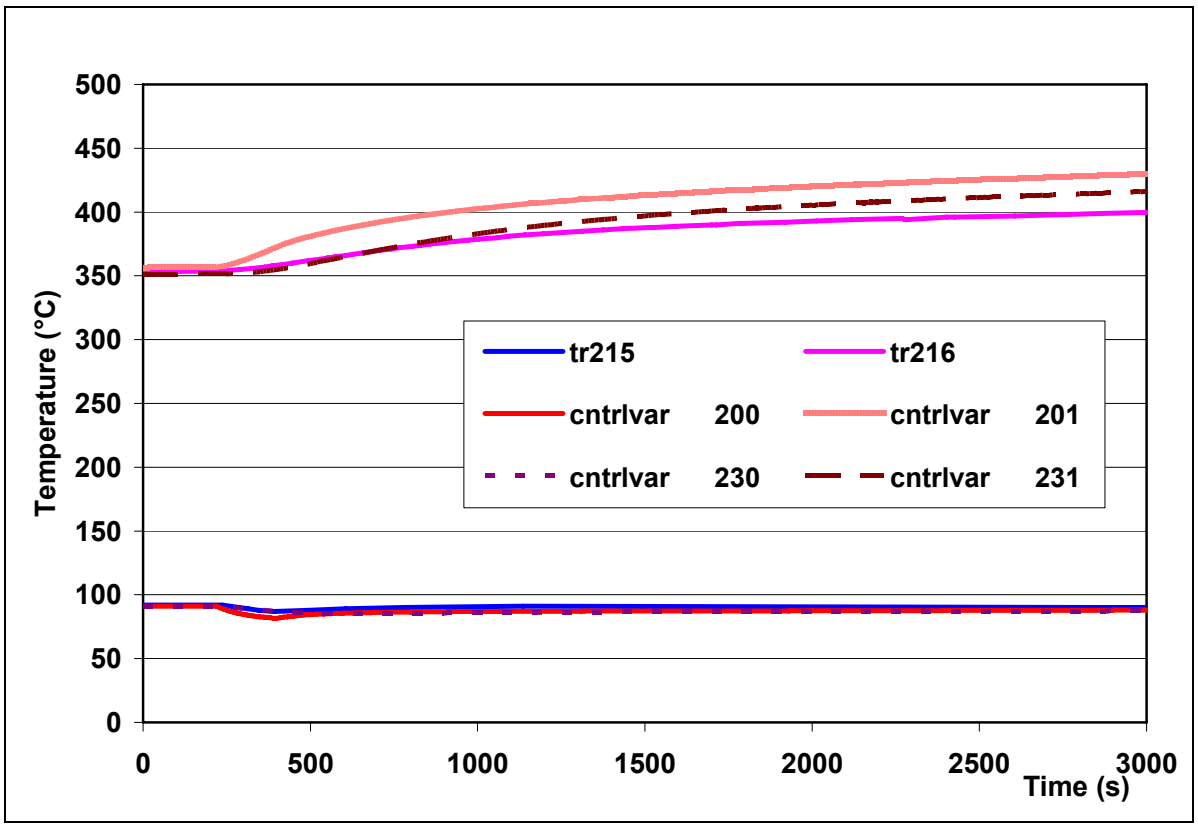

Fig. 4.27 – In and Out Economizer Cold Side Temperatures

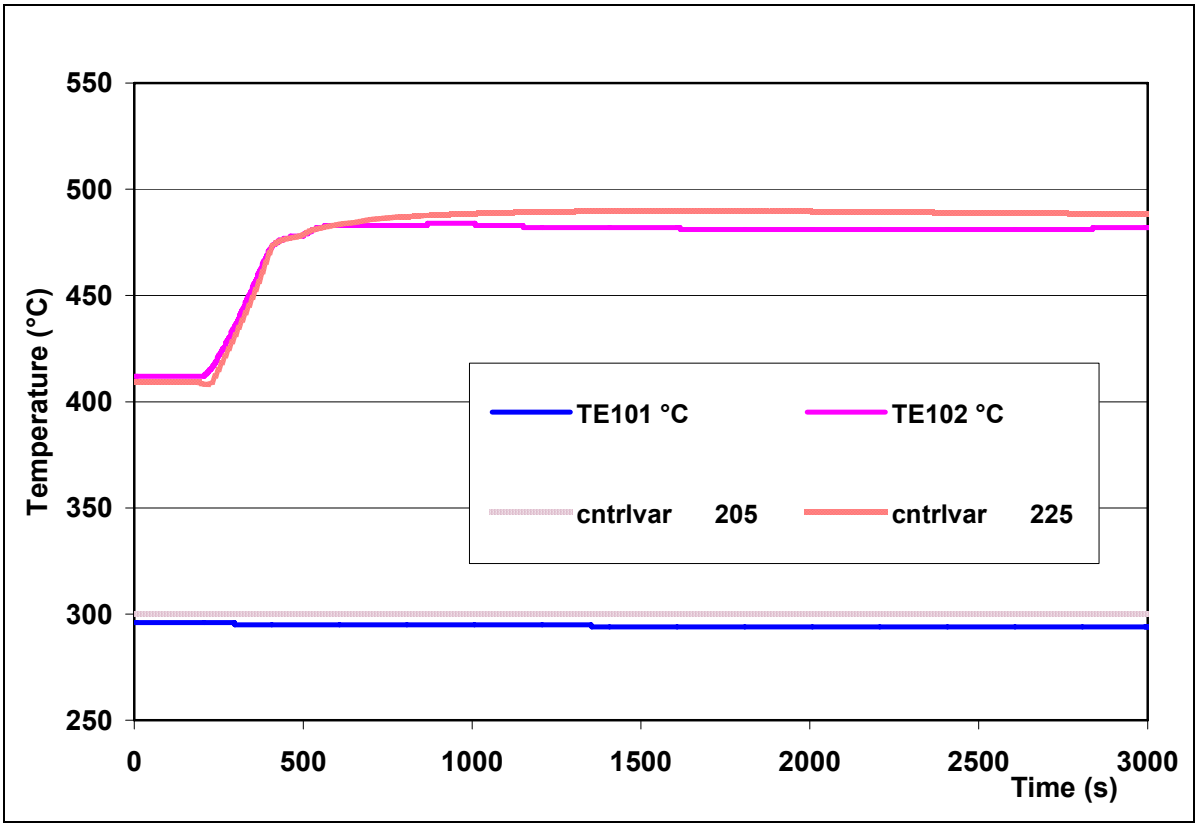

Fig. 4.28 – Inlet and Outlet TS Temperatures

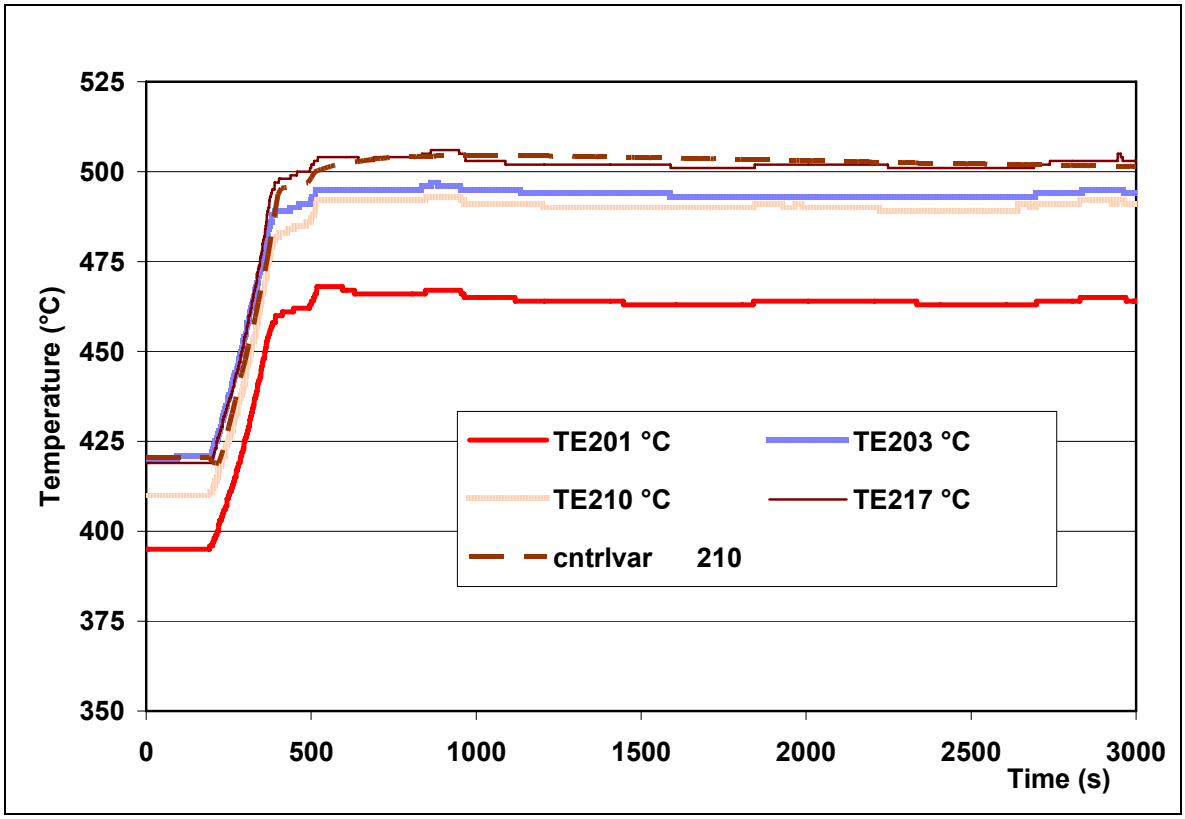

Fig. 4.29 – Pins 1-6 temperatures at 0.25 m

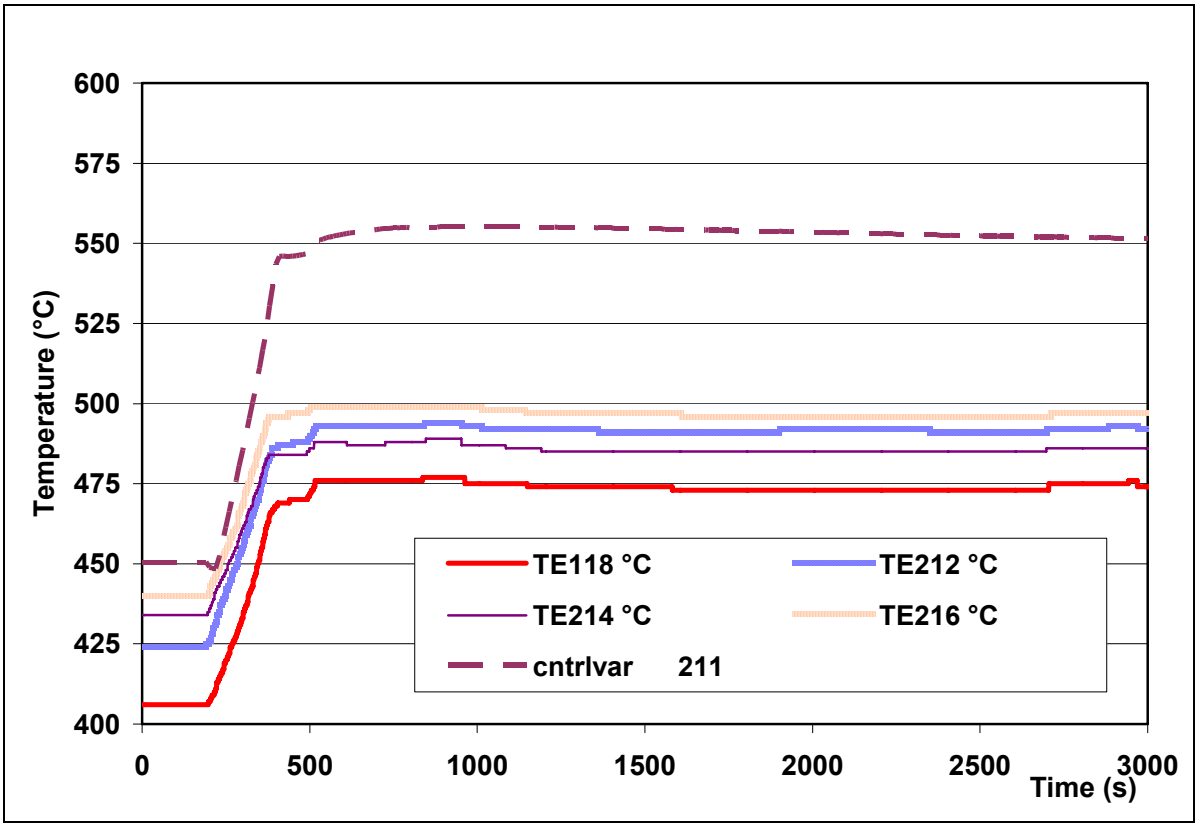

Fig. 4.30 – Pins 1-6 temperatures at 0.75 m

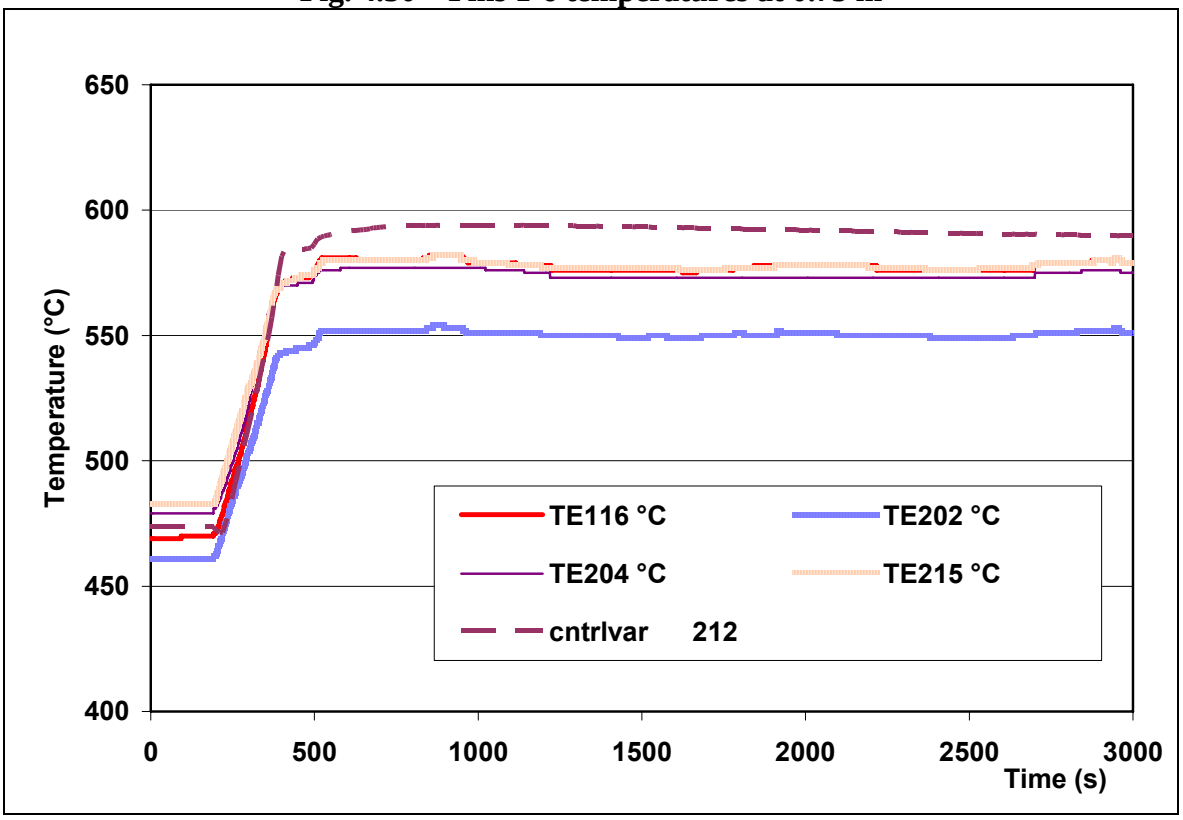

Fig. 4.31 – Pins 1-6 temperatures at 1.25 m

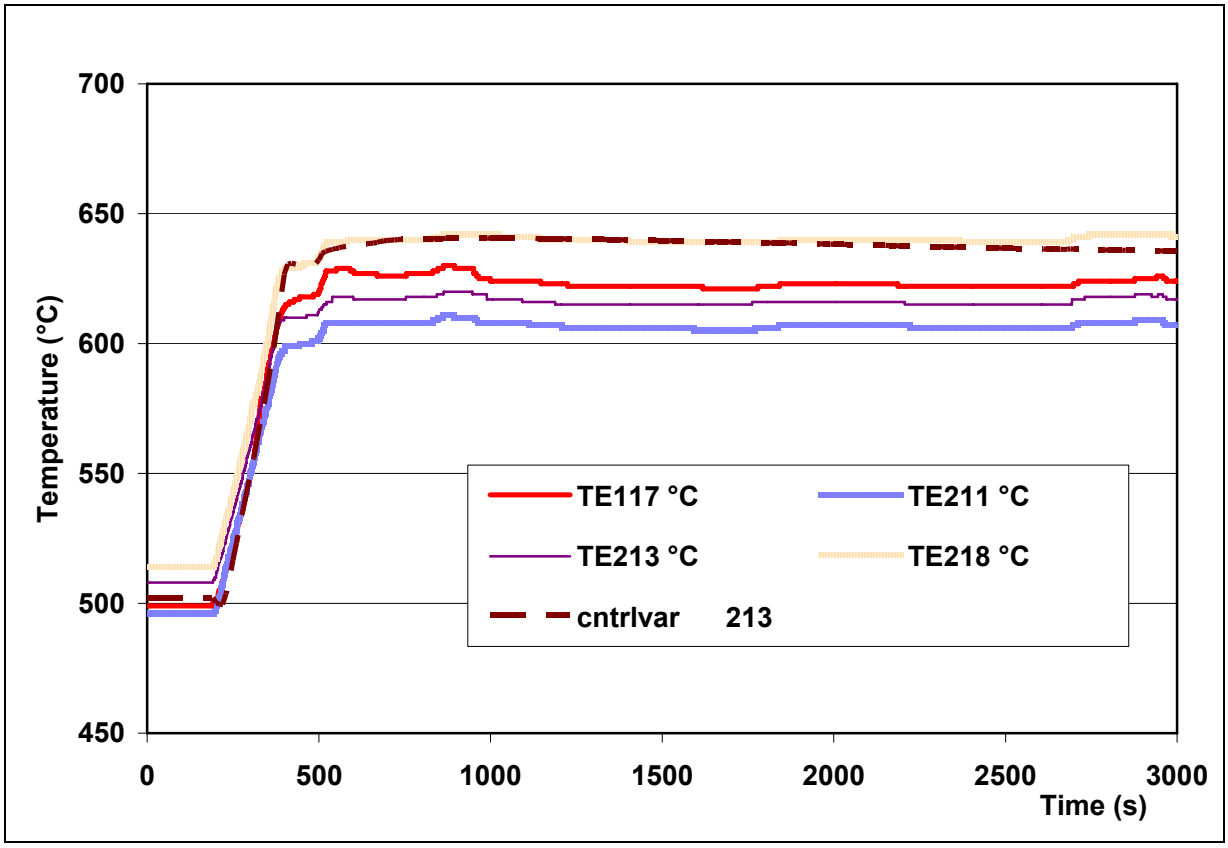

. Fig. 4.32 – Pins 1-6 temperatures at 1.75 m

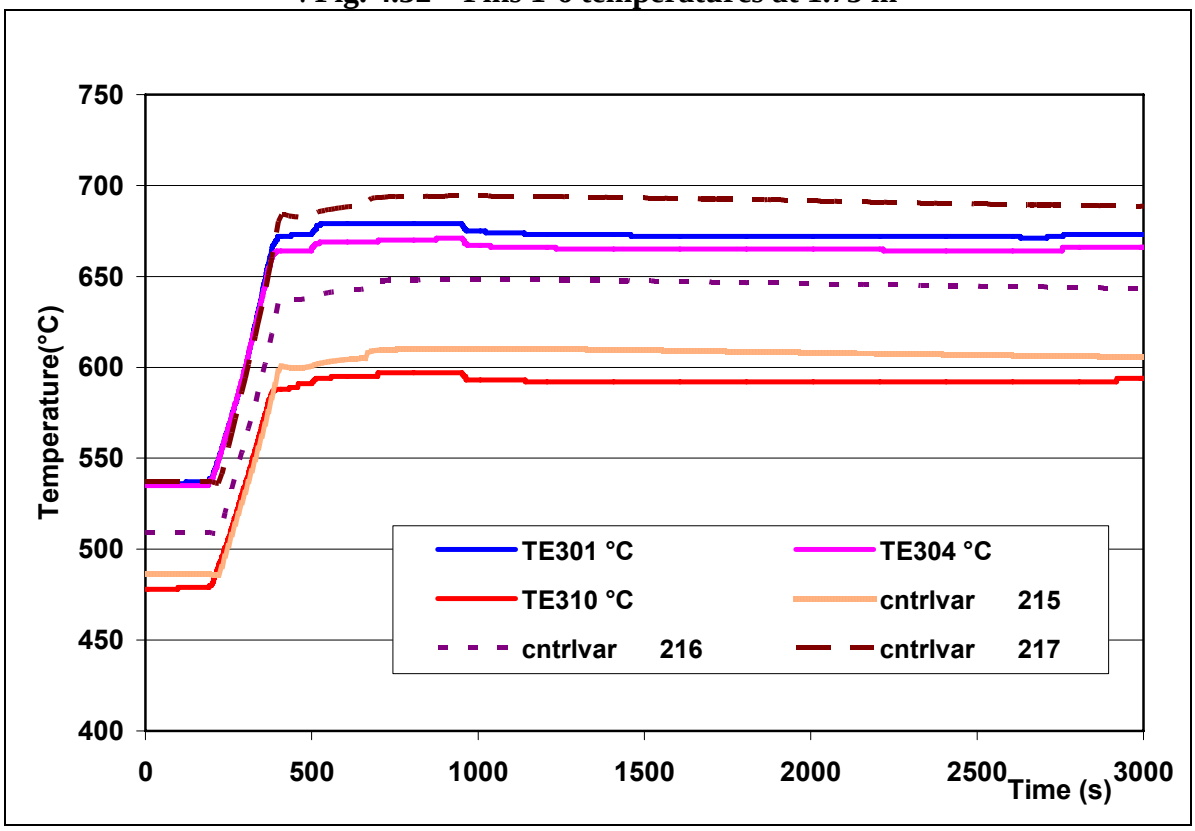

Fig. 4.33 – Pins 7 temperature at 0.75, 1.25 and 1.75 m

4.4 LOCA at 18 bar

The second LOCA transient was conducted starting from 18 bar, the stable pressure attained by the loop after the previous LOCA, with the same procedure of the previous one as described in § 2.3. The results of the post-test calculation for the main measured parameters are reported in Figs. 4.34 to 4.44 in comparison with the experimental data.

The boundary conditions used for the simulation of the transient conditions has been analogous to the previous LOCA: calibration of the break mass flowrate to obtain the experimental depressurization (Fig. 4.34)..

The situation for the loop mass flowrate (Fig. 4.35) and temperature (4.36 and 4.37) is very similar to the previous one and brings at the same conclusions. In this case, during the experimental transient, the inlet TS temperature remains below 300 °C without intervention of the by-pass valve 234. In the calculation, the incorrect simulation of the economizer efficiency, already well evident in the initial steady state conditions, brings to higher temperature in the hot part of the loop with the consequent operation of the valve to limit the TS inlet temperature below 300 °C.

This fact slightly influence the TS helium and pin temperatures (Figs. 4.38 to 4.43) but in general the trends are very similar to those already discussed for all previous transients.

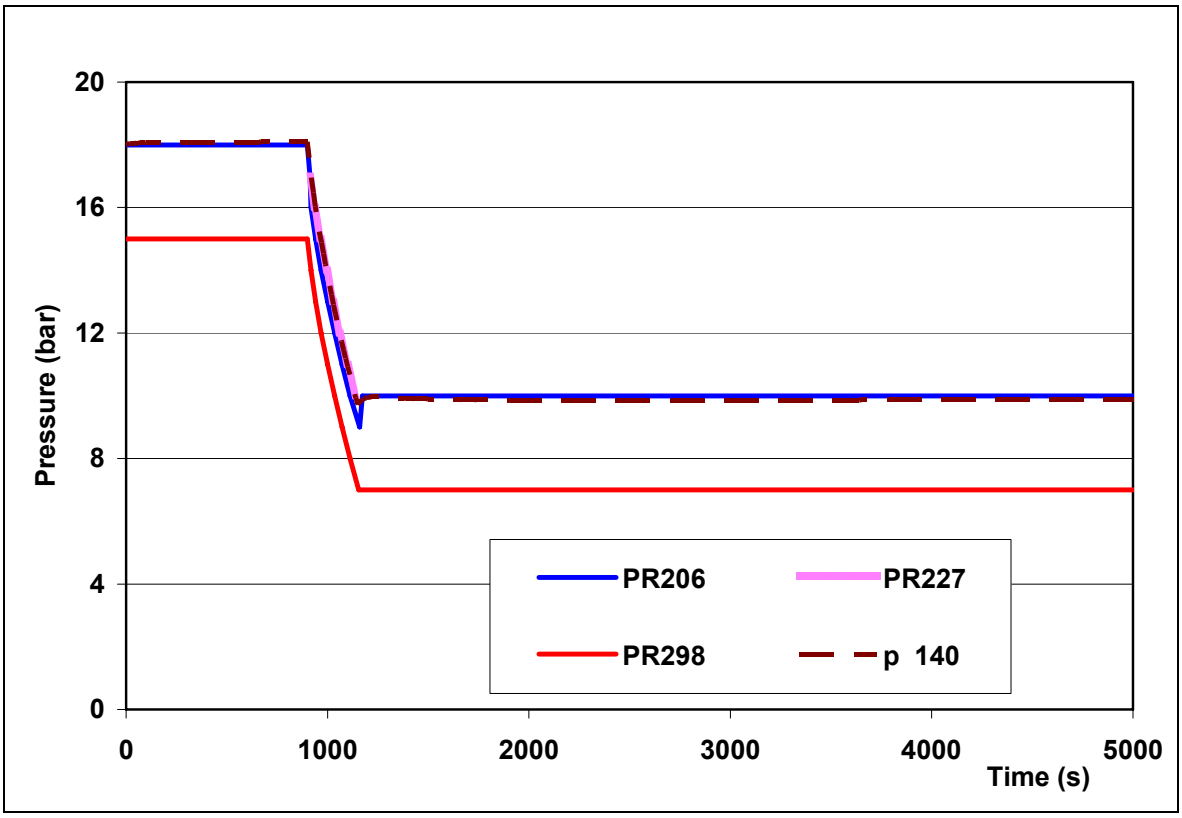

Fig.4.34 – Loop Pressures

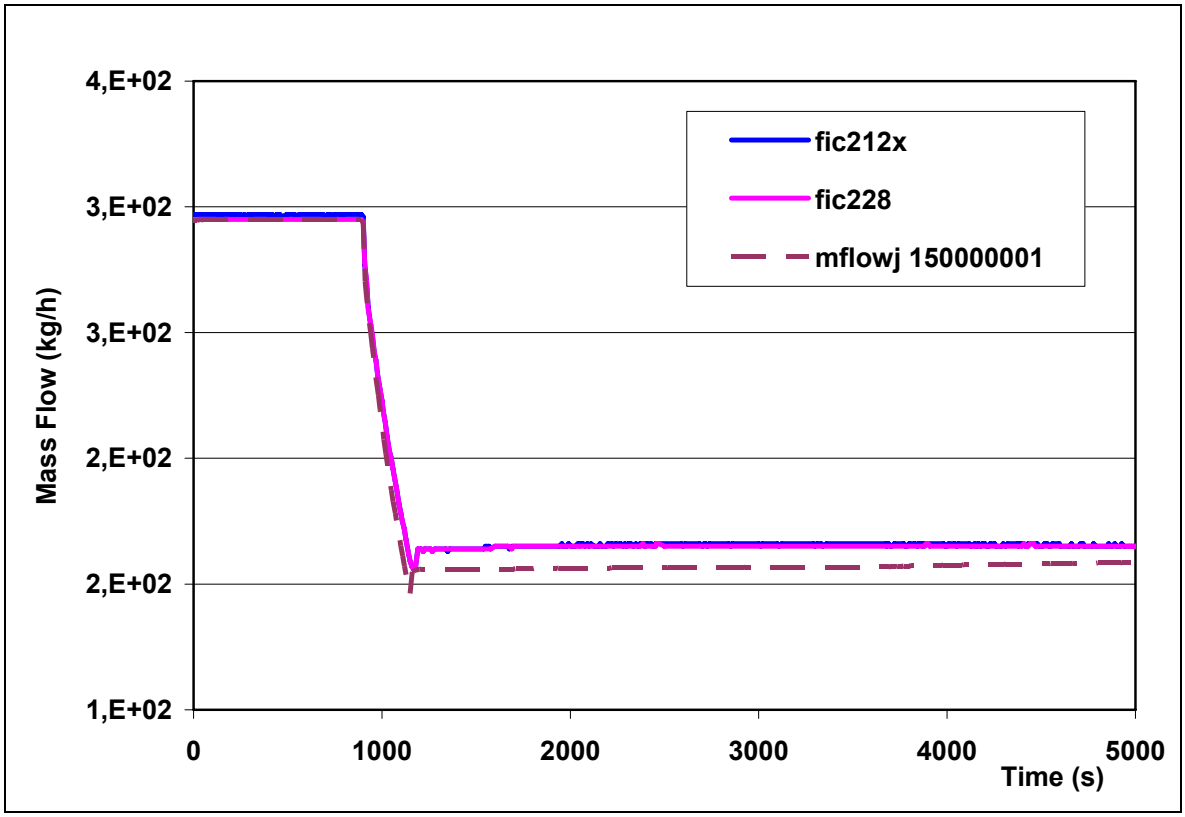

Fig. 4.35 –Loop Mass Flowrate

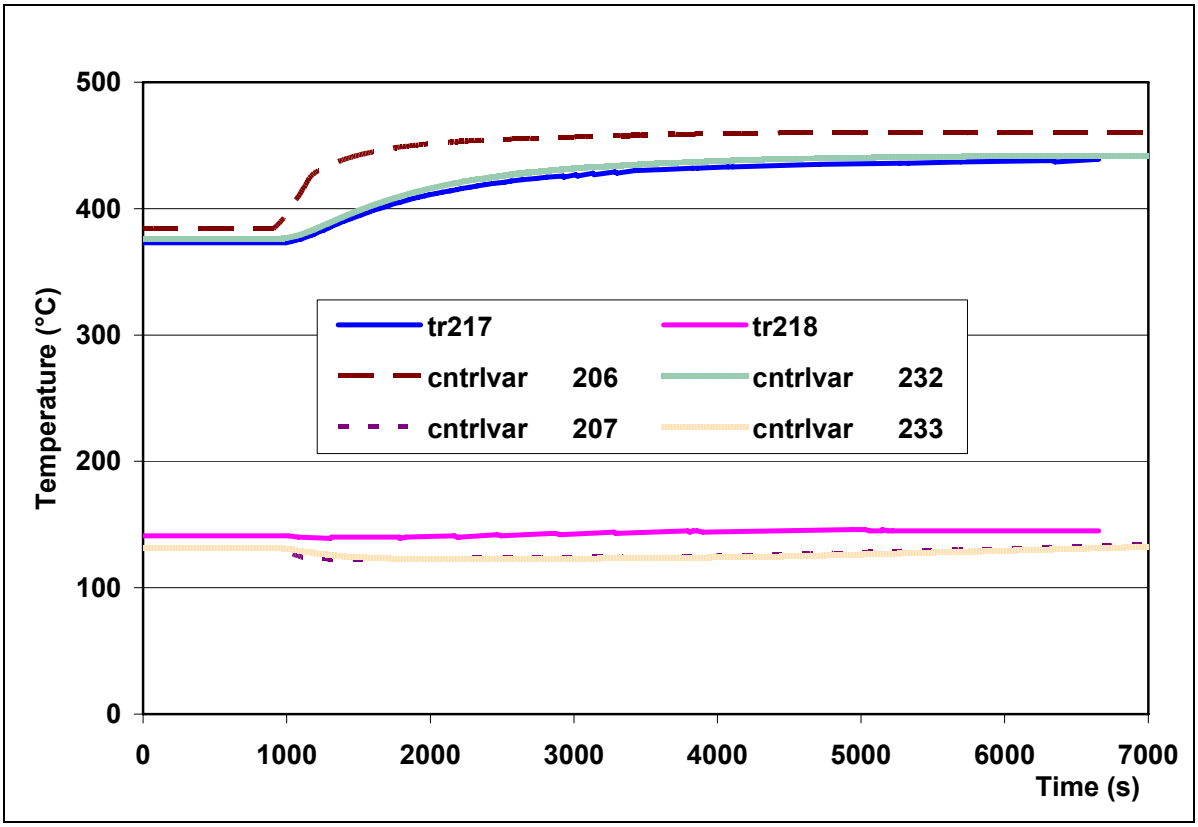

Fig. 4.36 – In and Out Economizer Hot Side Temperatures

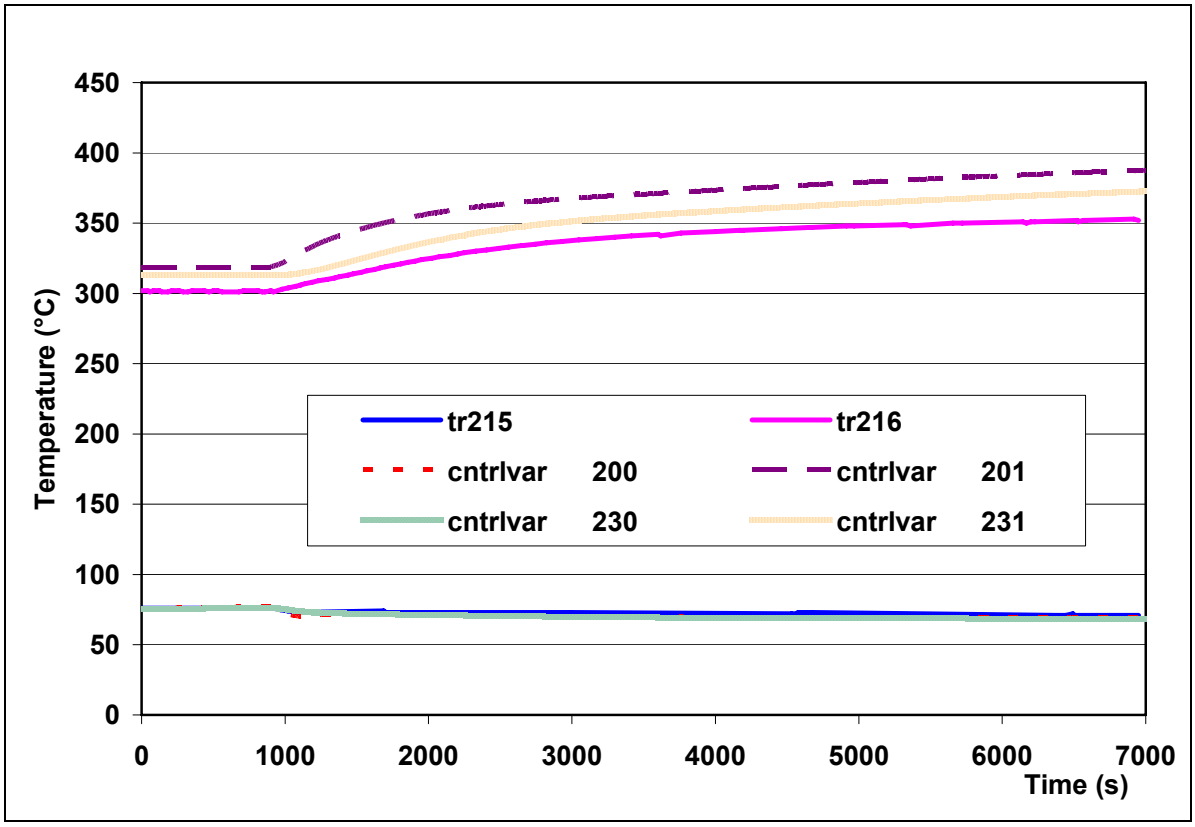

Fig. 4.37 – In and Out Economizer Cold Side Temperatures

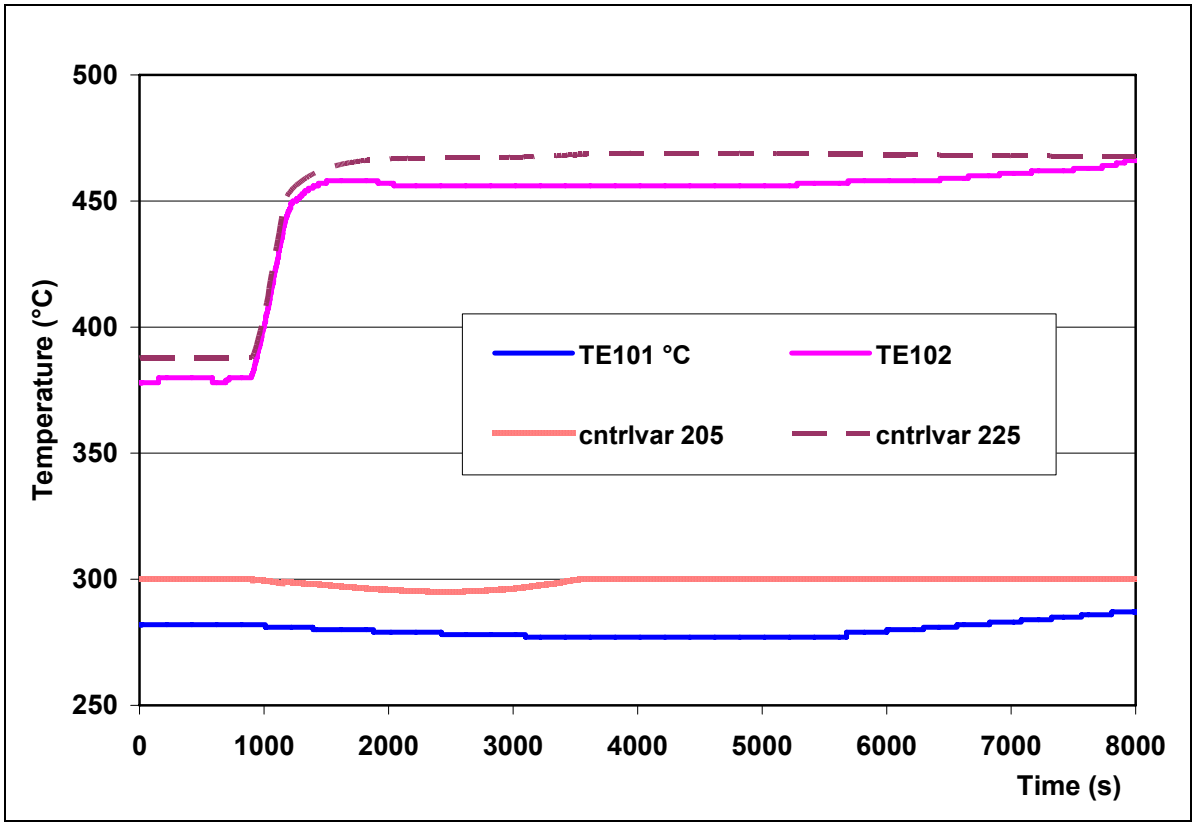

Fig. 4.38 – Inlet and Outlet TS Temperatures

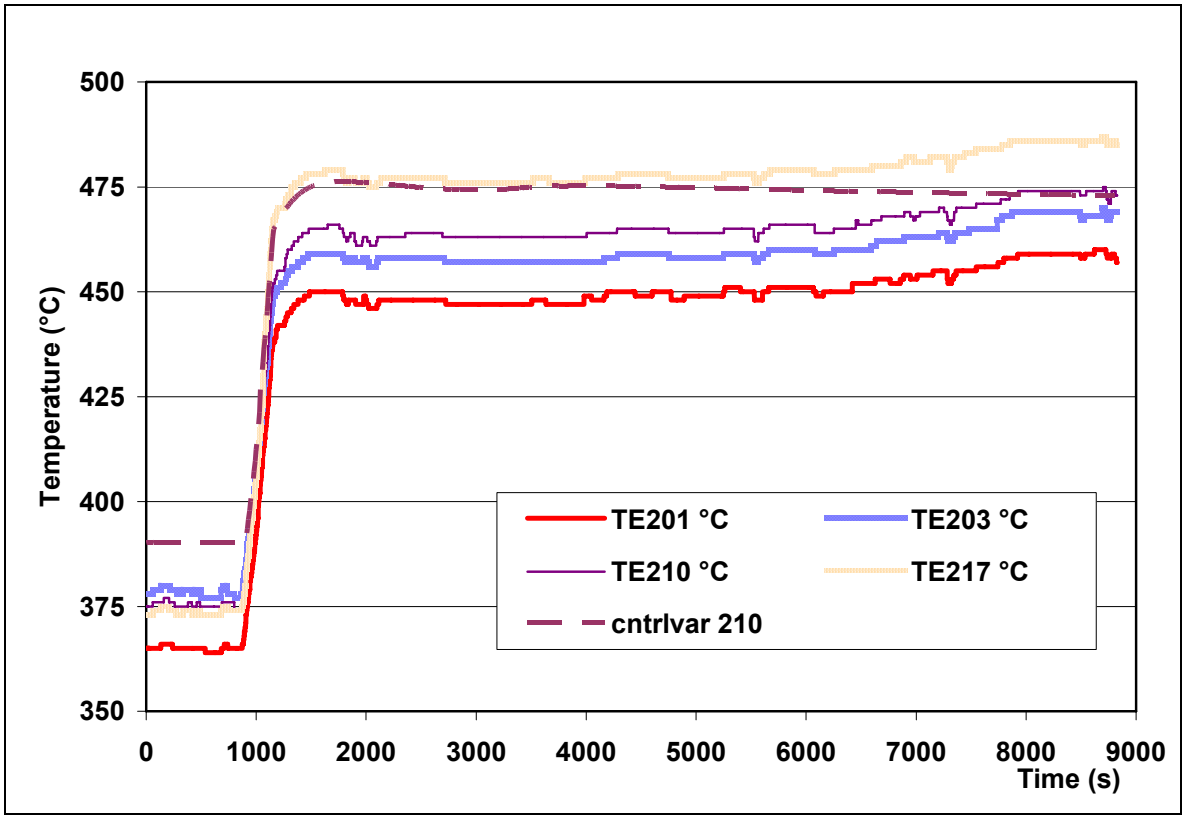

Fig. 4.39 – Pins 1-6 temperatures at 0.25 m

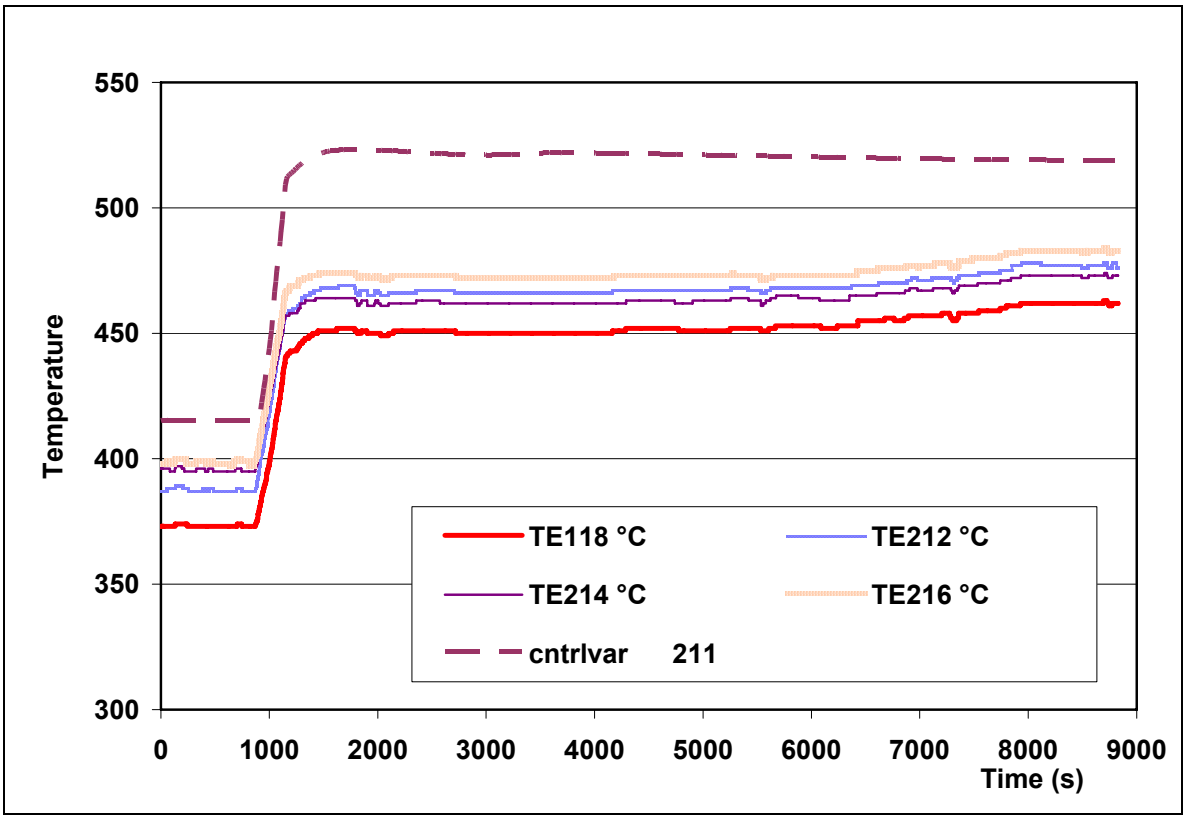

Fig. 4.40 – Pins 1-6 temperatures at 0.75 m

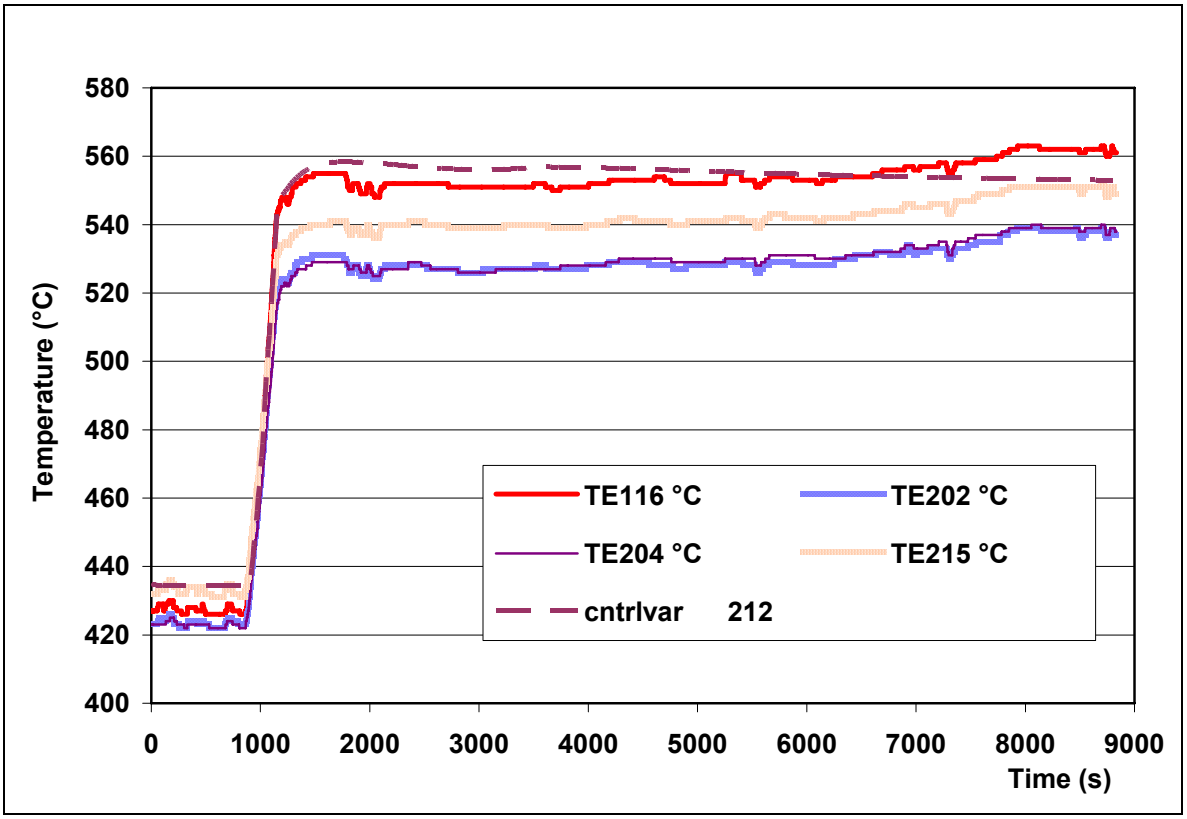

Fig. 4.41 – Pins 1-6 temperatures at 1.25 m

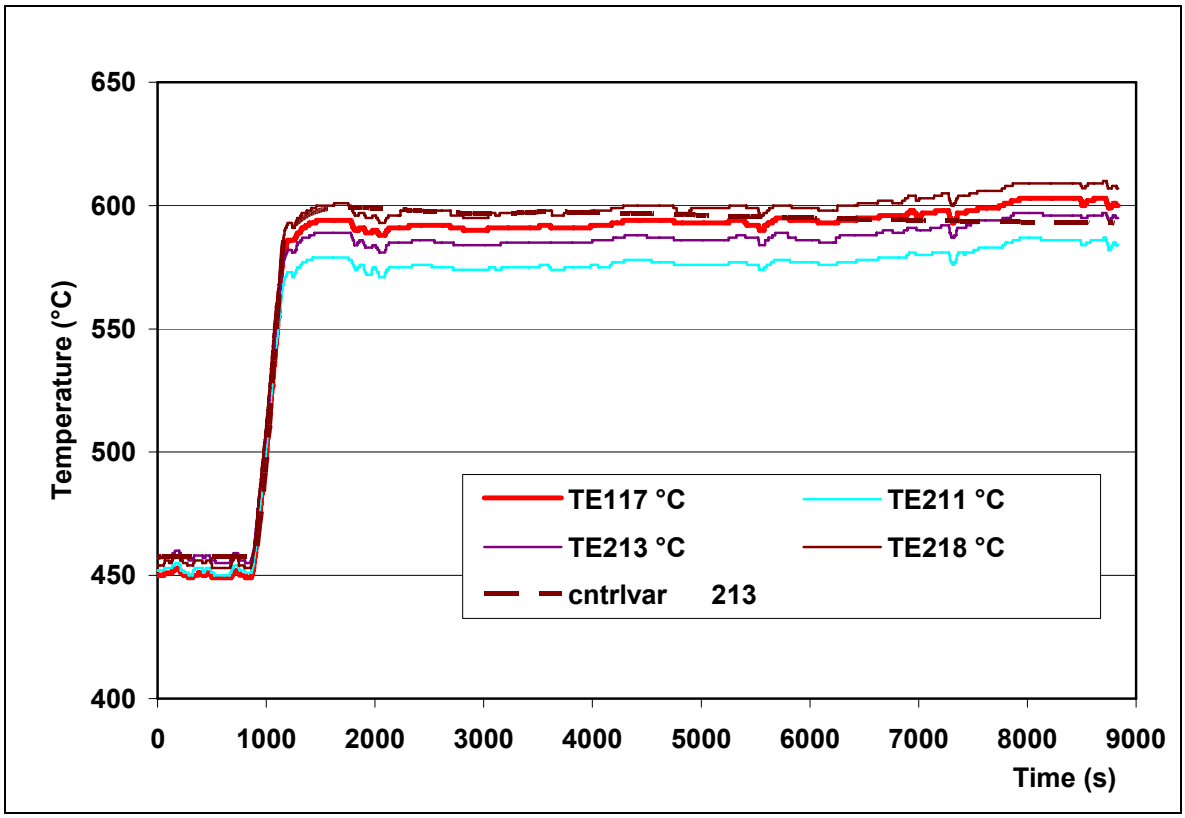

. Fig. 4.42 – Pins 1-6 temperatures at 1.75 m

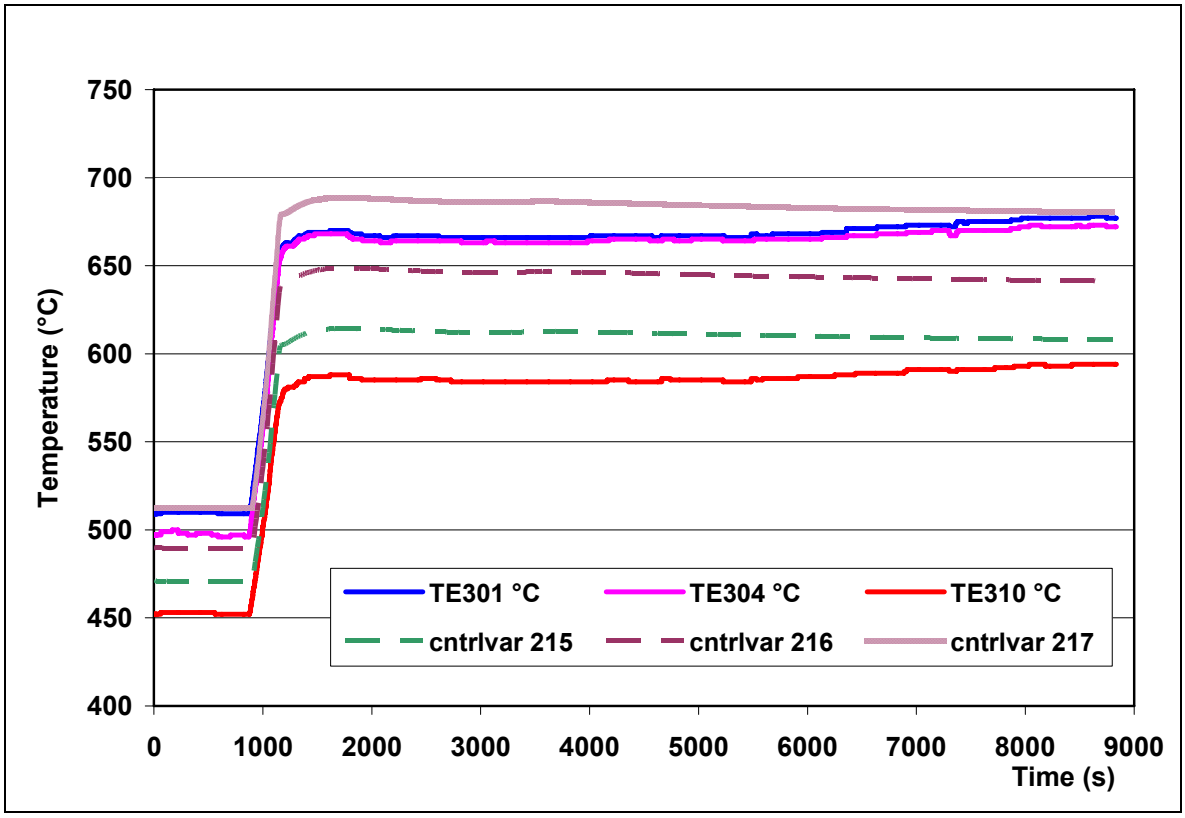

Fig. 4.43 – Pins 7 temperature at 0.75, 1.25 and 1.75 m

5. Conclusion

The post-test analysis of the recent HE.FUS3 experimental campaign performed with the RELAP5 loop model developed for the pre-test calculations has achieved two objectives:

- identify the necessary code developments and model improvements to be planned during the second year of the ENEA-MSE research program
- provide an evaluation of the experimental transients performed in order to fix the needs in term of further tests and additional instrumentation for the future experimental programs.

The post-test calculations of both steady state and transient tests have shown a general good capability of the RELAP5 model to simulate the thermal-hydraulic behaviour of helium cooled loop. The main discrepancies between calculation results and experiment data are related to the numerical modelling of the compressor and the economizer, which are the key components for the correct simulation of the HE-FUS3 loop behaviour.

From a point of view of the compressor modelling, the steady state and transient post-test calculation have highlighted the low reliability of the actual RELAP5 model based on the standard pump component in simulating the compressor behaviour in a large range of gas flow conditions. First at all, in order to provide a suitable set of homologous curves for the component there is the need to have sufficient and reliable experimental data matrix for the characterization of the component. It has been showed that the data produced in the previous experimental campaigns are not reliable, while the data produced in the recent campaign are for a limited range of conditions and incomplete due to the lack of the temperature measurement across the compressor, therefore additional dedicated test should be conducted to this aim. In parallel, starting from the data already available some modifications in the RELAP5 code should enlarge the range of the validity of the model respect to important variation of the loop pressure (i.e. helium density).

The present economizer model is not able to correctly reproduce the heat exchanger performance in all the loop conditions, however, the analyzed experimental campaign has made available sufficient experimental data for the development of a more suitable thermal exchange correlations to be implemented in RELAP5 within the framework of the future activity.

A number of open points remain as far as it concerns the loop instrumentation:

- The thermocouples along the loop do not provide a direct measurement of the helium temperature but they seem strongly influenced from the structure thermal capacity. New thermocouples directly immersed in helium should be installed, or a quantification of this influence should be provided in the future experimental activities.
- The 7-pin test section is carefully instrumented nevertheless important information about the position of the thermocouples and the acquisition of the signals is missed. This information should be recovered for an exhaustive analysis of the post-test results.

- The HE-FUS3 acquisition system of the instrumentation signals is not completely suitable for transient conditions, the acquisition frequency has to be increased in order to correctly monitor the system dynamics. Analogously, for some loop parameters (e.g. loop pressure) the accuracy of the measurement has to be strongly improved.
- Dedicated instrumentation have to be installed for the acquisition of essential information in particular transient conditions. For instance, in the LOCA transients conducted in the recent experimental activity any information about the break mass flowrate, which is an essential parameter for the interpretation of the transient, is missed.

5. References

[1] M. Polidori, "Final Report on HE-FUS3 Benchmark Exercise" , ENEA RT-FPN-P9L7-004, to be issued
.

[2] P. Meloni, "HE-FUS3 Experimental Campaign for the Assessment of Thermal-Hydraulic Codes: Pre-Test Analysis and Test Specifications" ENEA RT-FPN-P9LU-015, December 2008

[3] A. Tincani, L. Rapezzi, G. Polazzi, M. Querci, S. Panichi, "HE-FUS3 Experimental Campaign for the Assessment of Thermal-Hydraulic Codes: Experiment Data Report" ENEA RT-FPN-FISING-RG-T-R-002-Rev0 , April 2009

[4] M. Polidori "HE-FUS3 Loop: Data Sheets for Code Modelling and Experimental Data for Code Assessment", ENEA Document FPN – P9L7-001, April 2008